Advancing Monitoring and Mitigation of Antibiotic Resistance in Wastewater Treatment Plants and Water Reuse Systems

Haniyyah J. Majeed

Thesis submitted to the faculty of Virginia Polytechnic Institute and State University in partial fulfillment of the requirements for the degree of

Master of Science
in
Environmental Engineering

Amy J. Pruden, Chair
Marc A. Edwards
Peter J. Vikesland

September 22, 2020
Blacksburg, VA

Keywords: antibiotic resistance, wastewater treatment, wastewater reclamation

Advancing Monitoring and Mitigation of Antibiotic Resistance in Wastewater Treatment Plants and Water Reuse Systems

Haniyyah J. Majeed

ABSTRACT

Wastewater treatment plants (WWTPs) receive a confluence of sewage containing antibiotics, antibiotic resistant bacteria, antibiotic resistance genes (ARGs), and pathogens, thus serving as key point of interest for the surveillance of antibiotic resistance (AR) dissemination. This thesis advances knowledge about the fate of AR indicators throughout treatment and reuse.

The field study informs approaches for monitoring AR at a WWTP by characterizing the resistome (i.e., full profile of ARGs) and microbiome across eight sampling events via metagenomic sequencing, complemented by antibiotic data. The WWTP significantly reduced the total load of ARGs and antibiotics, although correlations between ARGs and antibiotics were generally weak. Quantitative polymerase chain reaction was applied to validate the quantitative capacity of metagenomics, whereby we found strong correlations. The influent and effluent to the WWTP were remarkably stable with time, providing further insight into the sampling frequency necessary for adequate surveillance.

The laboratory study examined the effects of commonly applied disinfection processes (chlorination, chloramination, and ultraviolet irradiation [UV]) on the inactivation of antibiotic resistant pathogens and corresponding susceptible pathogens in recycled and potable water. Further, we evaluated their regrowth following disinfection by simulating distribution. *Acinetobacter baumannii*, an environmental opportunistic pathogen, regrew especially well following UV disinfection, although not when a disinfectant residual was present. *Enterococcus faecium*, a fecal pathogen, did not regrow following any disinfection process. There were no significant differences between water types. The findings of this study emphasize a need to move beyond the framework of assessing treatment efficacy based on the attenuation of fecal pathogens.

Advancing Monitoring and Mitigation of Antibiotic Resistance in Wastewater Treatment Plants and Water Reuse Systems

Haniyyah J. Majeed

GENERAL AUDIENCE ABSTRACT

Wastewater treatment plants (WWTPs) have traditionally been designed and further enhanced to minimize environmental contamination caused by solid waste, fecal pathogens, nutrients (e.g., nitrogen), and organic matter. However, treatment has not been optimized to remove the contaminants of emerging concern (CECs) investigated in this thesis: antibiotic resistant bacteria (ARB), antibiotic resistance genes (ARGs), and antibiotics. WWTPs are key point of interest for local and global surveillance of antibiotic resistance as they can receive the aforementioned CECs (via human excretion or improper disposal) from various sources (e.g., residences, hospitals). Antibiotic resistant bacteria have caused 2.8 million infections and subsequently 35,000 deaths in the United States each year. Considering treated wastewater can serve as a route of exposure for humans, potential spread of antibiotic resistance by WWTPs is of high priority to mitigate from a public health perspective.

In the first study utilizing a technology to assess the full complement of ARGs in a given sample, we observed that the total load of ARGs was removed by approximately 50% across wastewater treatment, on average; total antibiotic load exhibited a similar reduction. The second study demonstrated that antibiotic resistant environmental opportunistic pathogen (i.e., pathogens which take advantage of the "opportunity" to infect an immunocompromised host, especially thriving in low nutrient engineered systems), *Acinetobacter baumannii*, possesses the ability to regrow following disinfection in the absence of a disinfectant residual. In contrast, antibiotic resistant *Enterococcus faecium*, an opportunistic pathogen of fecal origin, was successfully inactivated and unable to regrow. The findings of this study emphasize a need to move beyond the framework of assessing treatment efficacy based on the attenuation of fecal pathogens.

ACKNOWLEDGEMENTS

To Amy – thank you for giving me the push I needed to wrap up my thesis and have a successful defense. It has not been easy to balance finishing my graduate program and being a new mom, but you made it that much more bearable. Your dedication to the people you care for never ceases to amaze me; thank you for allowing me to be one of them.

To Marc – thank you for always making me feel as if I am exactly where I need to be, research-related or life-related. Your constant reassurance that I do not need to have the future completely mapped out has helped me live in the moment a little bit more and accept that no one has all the answers.

To Pete – thank you for attempting to help me maximize what time I had left of graduate school when you learned of my decision to leave soon. This is not something that was expected of you, but I have seen that this is what makes you special as an advisor.

To my colleagues – thank you all for being the most considerate group of people I have ever had the pleasure to work with. I am proud to call you all my friends.

To my mother, Tina – thank you for lighting the fire under me to keep pushing until I reach my full potential.

To the rest of my family and closest friends – thank you all for never making me feel as any goal I set for myself was unachievable.

To my husband, Nasif – thank you for all you have done to ease the burden of graduate school, especially since the baby arrived. You are my friend, my confidant, my biggest support and a pretty solid chef! I honestly could not have accomplished this achievement without you.

To the light of my life, Baby Luqman – thank you for hanging in there these past seven months while mama finished what she started. I hope I inspire you to do the same one day. In the meantime, I cannot wait to be able to hug and kiss you *all* day, *every* day now! Brace yourself.

TABLE OF CONTENTS

LIST OF FIGURES

LIST OF TABLES

CHAPTER 1: Introduction

Overview and Research Motivation

Wastewater treatment plants (WWTPs) have been designed to minimize environmental contamination caused by solid waste, pathogens of fecal origin, nutrients and organic matter. However, treatment has not traditionally been optimized to remove contaminants of emerging concern (Brodtmann & Russo, 1979; Lazarova et al., 1999). Specifically, this thesis focuses on antibiotic resistant bacteria (ARB), their antibiotic resistance genes (ARGs), and antibiotics in municipal wastewater and subsequent reuse.

Antibiotic resistant pathogens have caused greater than 2.8 million infections and 35,000 deaths in the United States each year (US CDC, 2019), making antibiotic resistance a top public health concern. WWTPs have the potential to be a critical point of mitigation of antibiotic resistance as WWTPs receive sewage containing residual antibiotics, corresponding resistant bacteria, and additional selective pressures (e.g., disinfectants, heavy metals) of various origins: domestic, clinical, commercial, and industrial. This is especially important from a public health perspective as discharge of treated wastewater, or unintentional discharges of untreated wastewater (e.g., storm events), into receiving water bodies (e.g., rivers, streams, lakes) used for drinking water or recreation could serve as a route of exposure for humans (Rizzo et al., 2013). Additional treatments may also be worthy of consideration upon recycling treated wastewater for potable or non-potable purposes.

Non-pathogenic bacteria also can carry ARGs; the concern being that non-pathogenic bacteria can share ARGs with pathogenic bacteria according to the following mechanisms of horizontal gene transfer: contact between live cells (i.e., conjugation; Salyers, 1995; Sorensen et al., 2005), uptake of extracellular DNA (i.e., transformation; Lorenz & Wackernagel, 1994), and via bacteriophages (i.e., transduction; Miller, 2001). Environments conducive to this genetic exchange, such as the highly microbially-active biological stage of treatment (i.e., activated sludge), are especially important for surveying the extent of which antibiotic resistance is spread.

Six multidrug resistant pathogens comprise the "ESKAPE" list, due to their tendency to "escape" the lethal effects of antimicrobials: *Enterococcus faecium, Staphylococcus aureus, Klebsiella pneumoniae, Acinetobacter baumannii, Pseudomonas aeruginosa*, and *Enterobacter* spp. (Rice, 2008). The United States Center for Disease Control and Prevention

(CDC) has categorized multiple antibiotic resistance pathogens according to their public health risk, including carbapenem resistant *Acinetobacter* and vancomycin resistant *Enterococci* listed as "urgent" and "serious" public health threats, respectively (US CDC, 2019).

Research Objectives

The goal of this research was to assess the extent of antibiotic resistance dissemination throughout wastewater treatment and potable reuse based on the fate and correlation of indicators of antibiotic resistance (i.e., ARB, ARGs, antibiotics).

Thesis Overview and Attributions

Chapter 1: *Introduction*

This chapter provides relevant background information and research motivation of the work completed in this thesis.

Chapter 2: *Temporal variation of the antibiotic resistome and microbiome at a conventional wastewater treatment plant assessed via repeated sampling*

This study reports the results of repeated sampling of a treatment train at a conventional WWTP, evaluating various dimensions of ARG selection by using shotgun metagenomic sequencing to profile the full "resistome," i.e., collective pool of ARGs carried across a microbial community. Core and discriminatory ARGs are identified and their patterns of removal or increase throughout treatment are characterized. The metagenomic data were assembled to identify evidence that ARGs occurred on mobile genetic elements or in pathogens and to compare patterns to local clinical resistance data. As part of a larger, global WWTP surveillance effort; this study provides insight into the sampling frequency needed to effectively capture differences in the resistome at a given WWTP for global versus local comparisons, and which stages of treatment and ARGs are most suitable as monitoring targets.

Attributions: Haniyyah J. Majeed led the writing of this chapter, co-written by Amy Pruden. Maria Virginia Riquelme, Benjamin C. Davis, and Peter J. Vikesland. Haniyyah J. Majeed, Maria Virginia Riquelme, Peter J. Vikesland, and Amy Pruden contributed to the experimental design. Benjamin C. Davis and Suraj Gupta contributed to the rationale of the metagenomic analysis approach. Luisa Angeles and Diana Aga conducted analysis of antibiotics. Jose Garcia, Ayella

Maile-Moskowitz, M. Storme Spencer, Mariah Gnegy, and Kris Mapili helped conduct sampling at the WWTP. Co-authors for this chapter are Maria Virginia Riquelme, Benjamin C. Davis, Suraj Gupta, Luisa Angeles, Diana S. Aga, Emily D. Garner, Amy Pruden, and Peter J. Vikesland.

Chapter 3: *Assessment of disinfection approaches for inactivation of antibiotic resistant Enterococcus faecium and Acinetobacter baumannii in potable reuse water*

This study evaluates the efficacy of three disinfectants (chlorine, chloramine, ultraviolet (UV) irradiation) for inactivation of *Enterococcus faecium* and *Acinetobacter baumannii* in a recycled water matrix. Multi-drug resistant and susceptible strains were implemented in this study to gain insight into potential strain differences. Further a re-growth period was implemented following disinfection to determine if the strains were able to recover and re-grow following disinfection. This study provides a benchmark, comparing the effects of the disinfectants at doses typical for recycled water for both a gram-positive and gram-negative pathogen, with comparison to efficacy of the same disinfectants added to drinking water to determine if there are potential interferences of the water matrix.

Attributions: This chapter was co-written by Haniyyah J. Majeed, E. Eldridge Hager Soto, and Amy Pruden. Disinfection experiments and culturing were performed by Haniyyah J. Majeed and E. Eldridge Hager Soto. Emily Garner, V. Jody Harwood, Marc Edwards, and Amy Pruden contributed to the experimental design. Jeanette Calarco contributed to the isolation and characterization of the strains used and provision and characterization of the waters used. Co-authors for this chapter are E. Eldridge Hager Soto, Ishi Keenum, Jeanette Calarco, Marc A. Edwards, Emily D. Garner, V. Jody Harwood, and Amy Pruden.

References

Lorenz, M. G. & Wackernagel, W. Bacterial gene transfer by natural genetic transformation in the environment, *Microbiol. Rev.*, 58, 563-602 **(1994)**.

Miller, R. V. Environmental bacteriophage–host interactions: factors contribution to natural transduction. *Antonie van Leeuwenhoek*, 79, 141-147 **(2001)**.

Rice, L. B. Federal funding for the study of antimicrobial resistance in nosocomial pathogens: no ESKAPE. *J. Infect. Dis.* 197, 1079-1081, doi:10.1086/533452 **(2008)**.

Rizzo, L., Manaia, C., Merlin, C., Schwartz, T., Dagot, C., Ploy, M. C., Michael, I., & Fatta-Kassinos, D. Urban wastewater treatment plants as hotspots for antibiotic resistant bacteria and genes spread into the environment: a review. *Sci Total Environ.* 447, 345−360, doi:10.1016/j.scitotenv.2013.01.032 **(2013)**.

Salyers, A. A. Conjugative transposons: an unusual and diverse set of integrated gene transfer elements. *Microbiol. Rev.*, 59, 579-590 **(1995)**.

Sorensen, S. J., Bailey, M., Hansen, L. H., Kroer, N., & Wuertz, S. Studying plasmid horizontal transfer *in situ*: a critical review. *Nat. Rev. Microbiol.*, 3, 700-710 **(2005)**.

US CDC. *Antibiotic Resistance Threats in the United States* **(2019)**.

CHAPTER 2: Temporal variation of the antibiotic resistome and microbiome at a conventional wastewater treatment plant assessed via repeated sampling

Haniyyah J. Majeed, Maria Virginia Riquelme, Benjamin C. Davis, Suraj Gupta, Luisa Angeles, Diana S. Aga, Emily Garner, Amy Pruden, and Peter J. Vikesland

Abstract

Wastewater treatment plants (WWTPs) receive a confluence of sewage containing antibiotics, antimicrobials, antibiotic resistant bacteria, antibiotic resistance genes (ARGs), and pathogens and thus are a key point of interest for surveillance of antibiotic resistance. Monitoring WWTPs has the potential to inform with respect to the resistance status of the community served as well as the potential for ARGs to escape treatment and spread via receiving environments. However, there is lack of agreement regarding suitable sampling frequencies and monitoring targets to facilitate global comparison among local WWTPs. The objective of this study was to examine the variability of metagenomic-derived indicators of antibiotic resistance with repeated sampling of the influent and effluent of a conventional U.S. WWTP. Quantitative polymerase chain reaction was performed targeting candidate anthropogenic and clinical "indicator" ARGs, along with total bacterial 16S rRNA genes, to validate the metagenomic approach and assess quantitative capacity. Total ARG relative abundance was remarkably consistent across eight sampling events over an 18-month period, which is suggests that highly frequent sampling may not be necessary for global comparisons. Further, it was found that total ARG relative abundance and relative resistome risk scores consistently decreased in magnitude from the influent to the effluent, suggesting that these are suitable measures of efficacy of WWTPs in the attenuation of antibiotic resistance and its potential to spread. In general, qPCR and metagenomic measures of ARG relative abundance were strongly and positively correlated, supporting the use of metagenomic data for quantitative comparisons. Overall, this study provides insights into means by which metagenomic data collection and analysis can be analyzed to for global and local surveillance of antibiotic resistance in WWTPs.

Introduction

Antibiotic resistance is a complex, global health threat that must be acted upon both globally and locally. Wastewater treatment plants (WWTPs) are a promising point of surveillance

and mitigation, as they receive a confluence of sewage containing antibiotics, other antimicrobials, antibiotic resistant bacteria (ARB), antibiotic resistance genes (ARGs), and pathogens. However, clear guidance is lacking with respect to which stage(s) of wastewater treatment and which monitoring targets are most informative with respect to assessing the ARG content of a given sewage, the potential for ARGs to mobilize and spread, and the efficacy of WWTPs in reducing ARG loads and associated human health risks prior to discharge or reuse.

Recent research demonstrates that ARGs that enter a given WWTP are reflective of various attributes of the local population, including antibiotic use patterns and socioeconomic factors (Aarestrup & Woolhouse, 2020). These ARGs may exist on mobile genetic elements (MGEs), such as plasmids and transposons (Kim et al., 2014), which can facilitate their spread among different bacteria, including human pathogens. Further, they may vary in the clinical relevance of the antibiotic to which they encode resistance (e.g., front-line versus last-resort antibiotics) and may exist intracellularly (i.e., within ARB) or extracellularly as naked DNA that could potentially later be assimilated via transformation. Ideally, an effective surveillance scheme will serve to capture the breadth and depth of the full profile of ARGs as they shift through each stage of treatment, but also provide the ability to link the observed ARG patterns to clinical antibiotic resistance concerns, both on a local and global scale.

Conventional WWTPs rely on the dense, highly microbially-active biological treatment step of activated sludge to efficiently remove organic matter and attenuate pathogens present in sewage. This has brought about concern that the activated sludge stage of treatment may serve as a "hotspot" for the mobilization of ARGs (Zhang et al., 2009; Rizzo et al, 2013). This concern largely stems from the potential for the conditions of activated sludge to facilitate horizontal transfer of ARGs to pathogenic host bacteria (Zhang et al., 2011). Numerous studies have been reported in the literature tracking various ARB and ARGs through WWTPs (Yang et al., 2014; Ju et al., 2019). Shotgun metagenomic sequencing is a promising means to gain such insight, as it enables direct profiling of total ARGs representative of a given sample (i.e., the "resistome", Wright, 2007), without biases associated with culture or primer-directed gene amplification methods (e.g., quantitative polymerase chain reaction (qPCR) or qPCR array). However, metagenomic surveillance approaches suffer from "too much information" and the need for systematic means to meaningfully assess and compare resistomes (Hendriksen et al., 2019), both locally for a given WWTP with time, and globally with other WWTPs. The quantitative capacity

of metagenomics is also not well defined, which is important for informing human health risk assessment. Furthermore, consensus is lacking with respect to ideal locations within the WWTP to sample, frequency of sampling, and which ARG targets are most informative with respect to potential for ARGs to mobilize, efficacy of treatment for reducing ARGs, and relevance to human health risk assessment. Several studies focused on classifying sewage (Parnanen et al., 2019; Hendriksen et al., 2019; Riquelme et al., in preparation) and final effluent (Parnanen et al., 2019) by geographical region to predict antibiotic resistance burden. One study recently produced ninety-seven metagenomes spanning over a nine-year monthly sampling campaign focused on the activated sludge stage of a WWTP in Hong Kong (Yin et al., 2019). Generally, the authors found that the activate sludge resistome clustered based on 2-3 years of consecutive monthly samples, while there was no seasonal clustering observed. Whereas another study with repeat sampling in a Northern Portugal WWTP suggested that wastewater treatment mitigated antibiotic resistance based on the reduction in the number of individual ARGs, reads of ARGs, and percentage of hosts harboring ARGs associated with mobile genetic elements (Lira et al., 2020). However, again the issue of the quantitative capacity of metagenomics is raised, in addition to the repeatability in sampling campaign being quite limited (i.e., 3 times over a 4-month period).

The overarching objective of this study was to assess the potential for metagenomic-enabled surveillance of WWTP-borne antibiotic resistomes. This was achieved via repeated sampling through various stages of treatment at a conventional WWTP and evaluation and bench-marking of various dimensions of the resistome, factors associated with ARG selection (e.g., antibiotics) and mobility (e.g., associations with MGEs), and local clinical resistance information. Specifically we examined the core (i.e., the full complement of ARGs detectable across all treatment stages) and discriminatory (i.e., ARGs that separate the influent from effluent) resistomes, along with specific ARGs of clinical concern or that have been identified as "indicators" of anthropogenic sources of resistance and compared these to independent measurements via qPCR and reports of local clinical resistance data. Further, we examined assembled metagenomic data for evidence of carriage of ARGs on MGEs and in pathogens, as represented by resistome risk scores. The findings help inform with respect to sampling locations, frequencies, and targets suitable for local and global monitoring of antibiotic resistance flowing into and emanating from WWTPs.

Materials and methods

Site description, sample collection, and sample preservation

A small (3 million gallons per day [MGD]), conventional (anoxic/oxic process with enhanced nitrogen removal) WWTP serving a population of approximately 21,500 in southwestern Virginia, United States was subjected to bi-monthly sampling over the course of 18 months. The design capacity of the WWTP is 6 MGD, treating approximately 95% of municipal wastewater (as % of COD) and 5% pre-treated industrial wastewater. Two industries contribute to the inflow at the WWTP: (1) a machine and fabrication plant discharging an average of 15,000 gallons per day (GPD) and (2) environmental waste industry discharging an average of 1,600 GPD out of an allowed 14,000 GPD; however this industry's input varies greatly depending on weather conditions. Prior to discharge to a local river, the final effluent is subject to ultraviolet disinfection. Details about the 8 sampling events are provided in Supplementary Table 1.

Grab samples were collected using sterile materials at each stage of treatment following and stored on ice until further processing. Temperature, dissolved oxygen (DO), and pH were measured on site for each aqueous sample. Upon receipt at the lab, aqueous samples were divided in triplicate by mixing vigorously and subsequently measuring the same mass of water for each replicate prior to concentrating on a 0.22 µm mixed-cellulose ester membrane filter (Millipore, Billerica, MA). The volume of water (determined by mass) for the first replicate to clog the filter was recorded. Filters were folded and stored in a 50% ethanol solution in 2-mL O-ring tubes and preserved at -20°C. At a later date, the filters were torn into ~1 cm^2 pieces using sterile forceps, transferred to lysing tubes and DNA extraction was performed using a FastDNA SPIN Kit for Soil (MP Biomedicals, Solon, OH).

Shotgun metagenomic analysis

Twenty-two samples were selected for shotgun metagenomic sequencing, representing influent and secondary effluent (i.e., prior to disinfection) samples from each sampling event and a cross section of each WWTP process for representative summer (August 2018) and winter (February 2018) events. Sequencing was performed by Diversigen, Inc. (Houston, TX) on an Illumina NovaSeq 6000 utilizing the NexteraXT DNA Flex library preparation kit (Illumina, San Diego, CA). The target depth was 7 GB per sample, corresponding to approximately 47 million reads (2 × 150 paired-end). The samples were uploaded to the MetaStorm (Arango-Argoty et al.,

2016) pipeline whereby they were quality filtered (Supplementary Table 2) prior to annotation with the following databases: Comprehensive Antibiotic Resistance Database (CARD) version 2.0.1 (Jia et al., 2017) and Metagenomic Phylogenetic Analysis 2 (MetaPhlAn2) (Truong et al., 2015). The manual curation CARD output from MetaStorm was reported as relative abundance (i.e., ARG copies per copies of 16S rRNA). To determine calculated absolute abundance, relative abundance values were multiplied by 16S rRNA gene copies as determined via qPCR. Reads were assembled in MetaStorm using the IDBA-UD *de novo* assembler (Peng et al., 2012) according to default parameters to generate scaffolds for MetaCompare (Oh et al., 2018). MetaCompare is a tool developed to assess resistome risk associated with a given environment by assigning a relative resistome risk score and values to project each sample in a 3-dimensional hazard space by normalizing the co-occurrence of sequences identified as (1) ARGs, (2) ARGs and MGEs, and (3) ARGs, MGEs, and human pathogens to the total number of contigs. The core resistome of the influent and secondary effluent was determined as any ARG with a non-zero value relative abundance detected across all sampling events. ExtraARG (Gupta et al., 2019), established based on the extremely randomized tree algorithm, was utilized to identify discriminatory ARGs (i.e., ARGs that collectively distinguish different wastewater samples) taking relative abundance into account.

Quantitative polymerase chain reaction

All quantitative polymerase chain reaction (qPCR) assays were performed on a CFX96 Real Time System (BioRad, Hercules, CA) on triplicate DNA extracts. Gene copies of total bacterial 16S rRNA genes (Suzuku, Taylor, & Long, 2000) and the following "indicators" of ARGs of anthropogenic and clinical relevance were quantified based on previously published protocols: *bla*TEM (Bibbal et al., 2007), *erm*B (Chen et al., 2007), *sul*1 (Pei et al., 2006), *van*A (Dutka-Malen, Evers, & Coruvalin, 1995), and *int*I1 (Hardwick et al., 2008). A 100-fold dilution was determined as optimal to minimize inhibition and applied to the corresponding influent, secondary, and final effluent DNA extracts. On each qPCR plate, a triplicate negative control and standard curve ranging from 10^7 to 10^1 gene copies/µL were included for each target gene.

Seasonality

To further explore seasonality, samples separated from the influent (n = 8) and secondary effluent (n = 8) and grouped by two sampling events in each season, winter (ambient temperature

range = 3-19°C, influent temperature range = 11.8-14.1°C, secondary effluent temperature = 12.7°C), spring (ambient temperature range = 16-21°C, influent temperature range = 14-20°C, secondary effluent temperature range = 14.8-20.8°C), summer (ambient temperature range = 22-24°C, influent temperature range = 20.6-22°C, secondary effluent temperature range = 23.1-23.2°C), and fall (ambient temperature range = 11-13°C, influent temperature range = 18.6-19.8°C, secondary effluent temperature range = 18-20.1°C). Influent and secondary effluent samples were also separated into grouped seasons as such: winter/spring (average ambient temperature = 14.75°C, average influent water temperature = 14.98°C, average secondary effluent water temperature = 15.25°C) and summer/fall (average ambient temperature = 17.5°C, average influent water temperature = 20.25°C, average secondary effluent water temperature = 21.1°C) to capture a gradual transition from one extreme season (i.e., summer or winter) to the next.

Antibiotic analysis

Aqueous samples were subject to solid phase extraction and the cartridges shipped to the at the University at Buffalo for ultraperformance liquid chromatography-tandem mass spectrometry (UPLC-TMS) analysis of the following antibiotics: acetylsulfamethoxazole, anhydro erythromycin, anhydrochlorotetracycline, azithromycin, chlorotetracycline, ciprofloxacin, clarithromycin, erythromycin, enrofloxacin, norfloxacin, oxolinic acid, oxytetracycline, roxithromycin, sarafloxacin, spiramycin I, spiramycin II, spiramycin III, sulfachloropyrazidine, sulfadiazine, sulfamethoxine, sulfamerazine, sulframethazine, sulfamethizole, sulfamethoxazole, sulfamethoxydiazine, sulfathiazole, tetracycline, tilmicosin, trimethroprim, and tylosin. Water samples were collected in pre-combusted (at a temperature of 500°C) amber glass bottles for antibiotic analysis. The methods applied were as described previously (Singh et al., 2019). As the selected protocol for solid phase extraction and downstream UPLC-TMS required the use of amber glass bottles to collect water samples at the treatment plant, the ability to detect tetracyclines was lost due to their tendency to sorb to glass.

Statistical analysis and data visualization

To determine differences between stages of treatment, a paired Wilcoxon rank-sum test was utilized using the wilcox.test() in R version 3.5.1 (R Core Team, 2018) with the built-in stats package. One-way analysis of similarities (ANOSIM) based on Bray-Curtis dissimilarity was conducted in R using the anosim() function from the vegan (Oksanen et al., 2019) R package to

compare differences among groups based on sampling event, stage of treatment, and seasonality. Procrustes analysis was conducted using the procrustes() function in the vegan R package. Correlation analyses were performed using the Spearman option in rcorr() contained within the Hmisc R package. A significance level of $\alpha = 0.05$ was used for all statistical analyses. Nonmetric multi-dimensional scaling analysis was applied to visualize and compare relative abundances of ARGs and taxonomic ranks across samples. All graphics were generated using ggplot2 (Wickham, 2016) and RColorBrewer (Neuwirth, 2014) in R.

Results

Trends in Total ARG Relative Abundance from Influent to Effluent

A total of 953 ARGs, annotated against CARD version 2.0.1 (Jia et al., 2017), were identified across all 22 samples collected over eight sampling events. ANOSIM analysis confirmed that there was a distinct shift in the resistome composition from influent to effluent, while there was no significant separation between the secondary versus final effluent (Supplementary Table 4, Supplementary Table 5). Secondary and final effluent samples were thus grouped together for subsequent analysis, as applicable. Our choice to examine secondary effluent establishes a baseline representation of wastewater treatment, as final disinfectant treatment processes differ across various plants.

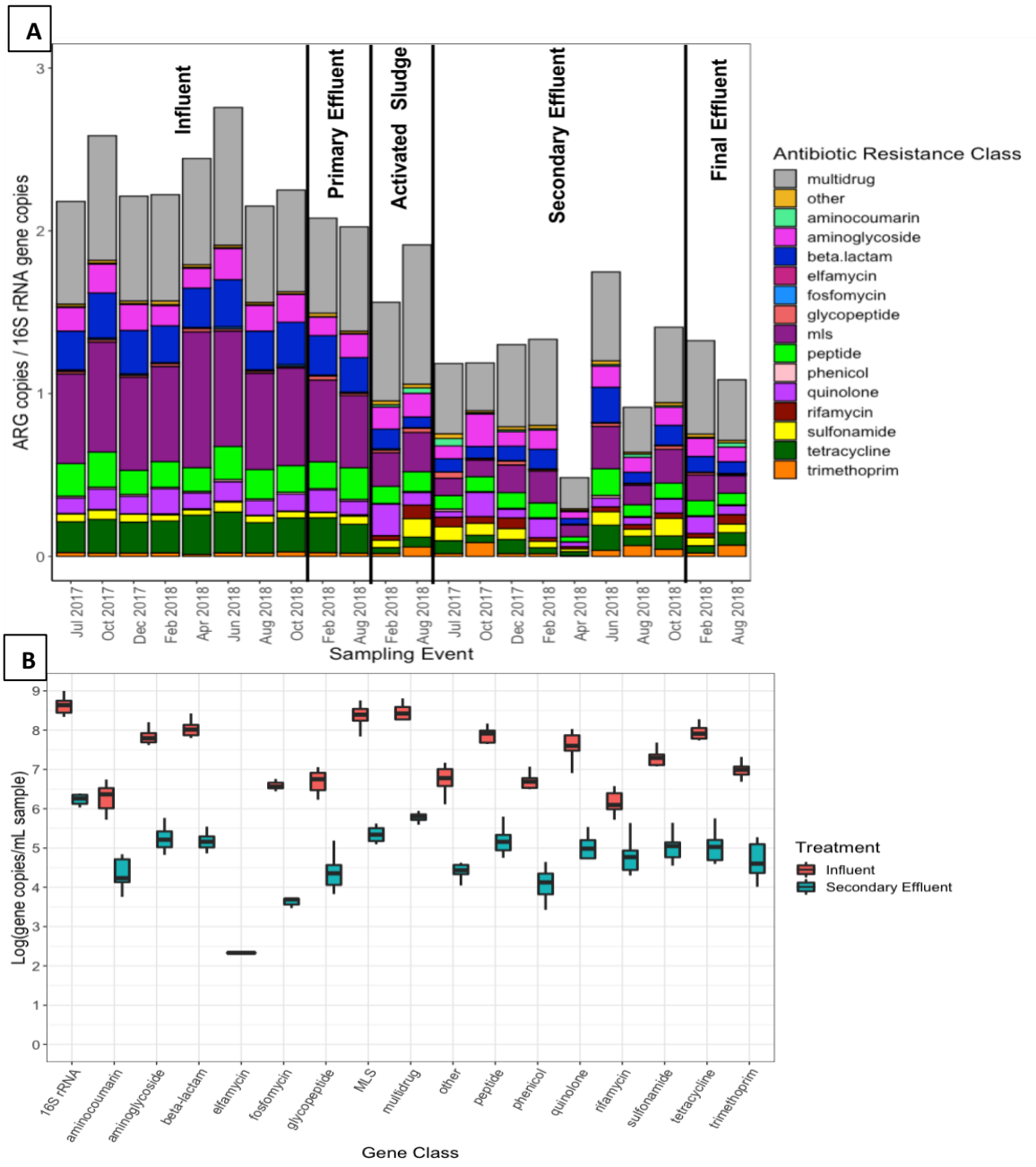

Figure 2-1. Metagenomic characterization of ARGs detected in all samples grouped by resistance class.

Total ARG relative abundance (copies per copies of 16S rRNA normalized as previously described [Li et al., 2015]) across all 22 samples **(A)** and calculated absolute abundance (relative abundance multiplied by 16S rRNA gene copies quantified by qPCR) **(B)**. ARGs were identified via annotation against CARD version 2.0.1 (Jia et al., 2017). "Multi-drug" represents ARGs conferring resistance to antibiotics corresponding to at least two drug classes, whereas the "other" category comprises genes conferring resistance to non-antibiotics (e.g., antimicrobials, antifungals).

There were 859 ARGs detected across all influent samples and an average total ARG relative abundance (i.e., per 16S rRNA gene copies) of 2.35 (minimum = 2.15, maximum = 2.76) (Figure 2-1). ARGs corresponding to the following classes represented the majority of ARGs detected: multidrug (26.7-30.7% of total ARGs), macrolide-lincosamide-streptogramin (MLS, 25.3-34.1%), and beta-lactam (9.9-12.4%) antibiotics (Figure 2-1). In secondary effluent samples, there were 637 ARGs detected and an average total ARG relative abundance of 1.20 (minimum = 0.48, maximum = 1.75). ARGs corresponding to the following resistance classes were most abundant: multidrug (24.7-39.6% of total ARGs), MLS (8.6-14.9%), aminoglycoside (6.6-16.7%), beta-lactam (6.1-12.4%) and quinolone (3.0-12.4%) antibiotics (Figure 2-1). For each sampling event, there was a decrease in total ARG relative abundance from influent to secondary effluent (Wilcoxon, paired; p = 0.007813), corresponding to an average removal of 1.15 ARG copies/16S rRNA gene copies or approximately 50% removal (Figure 2-1). 16S rRNA gene copies per mL sample decreased more than 2-log from influent to secondary effluent, resulting in a similar log-reduction per resistance class (Figure 2-1).

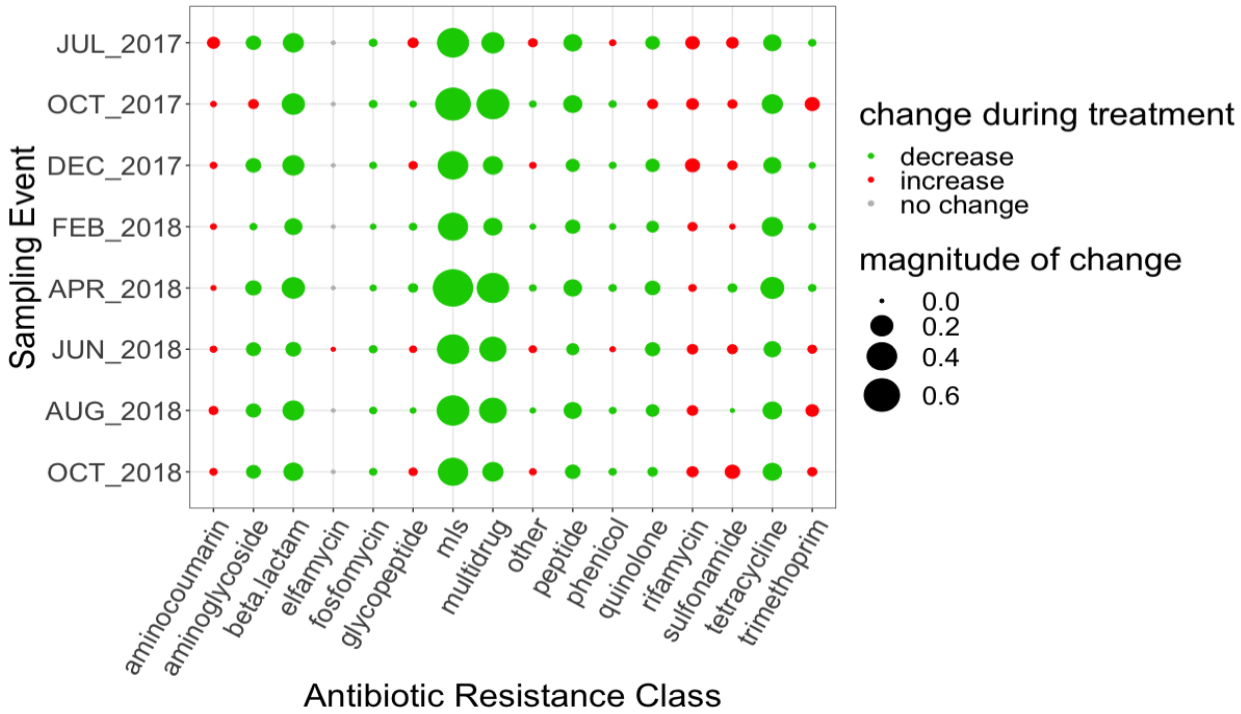

Figure 2-2. Magnitude of change in relative abundance of ARGs aggregated by resistance class.

Change was calculated as the difference between the relative abundance of the secondary effluent and the relative abundance of the influent.

The absolute magnitude of change between the influent to the secondary effluent by antibiotic resistance class ranged between 8.15×10^{-5} to 0.76 ARG copies/16S rRNA gene copies (Figure 2-2). ARGs belonging to the MLS resistance class decreased to the greatest extent, with an average removal of 0.49 ARG copies/16S rRNA gene copies. However, there was an increase in relative abundance of ARGs conferring resistance to several classes through the secondary clarification process: aminocoumarin (8/8 sampling events), glycopeptide (4/8), phenicol (July 2017, June 2018), rifamycin (8/8), sulfonamide (6/8), trimethoprim (4/8), and other (4/8) antibiotics (Figure 2-2).

Fate of core and discriminatory ARGs identified in the influent and effluent

Table 2-1. Top 25 most abundant core influent ARGs, based on mean relative abundance, that were also detected in secondary effluent.

Antibiotic Resistance class	**Antibiotic Resistance Genes**
aminocoumarin	*par*Y in *Streptomyces rishiriensis*
aminoglycoside	*aac*(6')-Ib7
beta-lactam	*oxa*-210
MLS	*mac*B, *mph*D, *mph*G, *msr*B, *msr*E, *erm*B, *erm*F
peptide	*pmr*E, *ros*B
quinolone	*qac*H, *qnr*S2
sulfonamide	*sul*1, *sul*2
tetracycline	*tet*39, *tet*Q
multidrug	*ade*J, *ade*K, *cpx*R in *Pseudomonas* aeruginosa, *crp*, *mdt*B, *mex*K, *msb*A, *mux*B

Table 2-2. Top 25 most abundant secondary effluent ARGs, based mean relative abundance, that were also detected in the influent core resistome.

Antibiotic Resistance class	**Antibiotic Resistance Genes**
aminocoumarin	*par*Y in *Streptomyces rishiriensis*
aminoglycoside	*aac*(6')-Ib7, *aac*(6')-Ib8, *kdp*E

MLS	*mac*B, *mph*D, *msr*B, *msr*E
peptide	*pmr*E, *ros*B
quinolone	*qac*H, *qnr*S2
sulfonamide	*sul*1, *sul*2
multidrug	*ade*F, *cpx*R in *Pseudomonas* aeruginosa, *crp*, *mdt*B, *mdt*C, mexK, *msb*A, *mux*B, *mtr*A, *sme*R, *oqx*B
Other	*ile*S in bifidobacteria

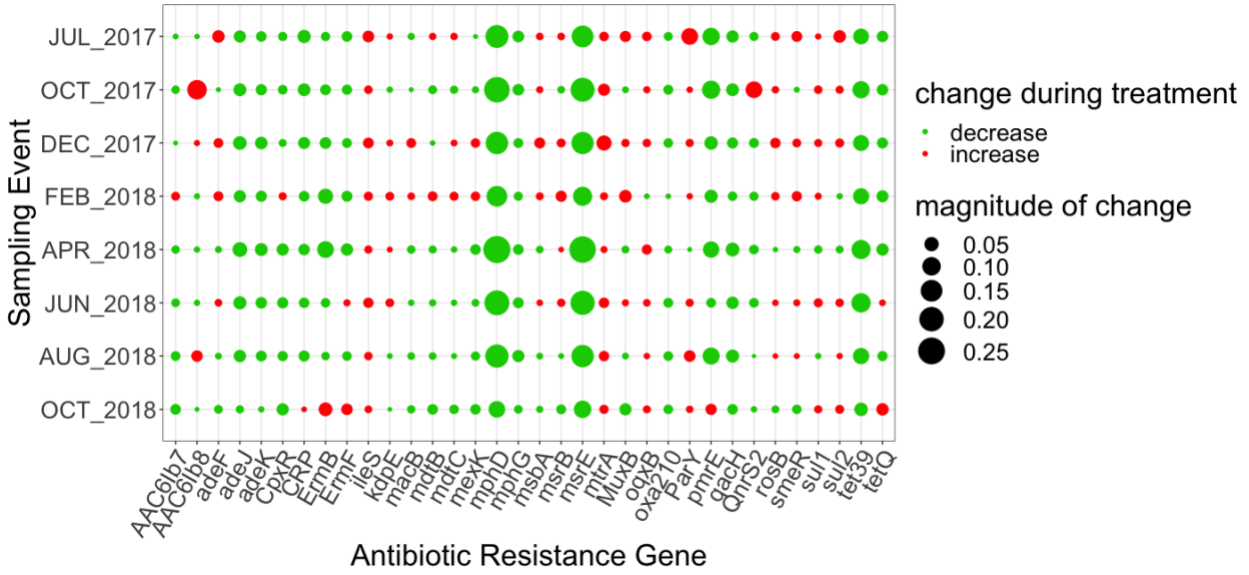

Figure 2-3. Magnitude of change in relative abundance between influent and secondary effluent of top 34 ARGs pertaining to the core resistome.

The core WWTP resistome was defined as consisting of ARGs detected across each treatment process and all sampling events; this resulted in 111 core ARGs identified. However, there were 143 ARGs detected in both the influent and secondary effluent during each sampling event. The top 25 most abundant of these in the influent based on mean relative abundance are presented in Table 2-1. The top 25 most abundant of these in the effluent based on mean relative abundance are presented in Table 2-2. The top 25 ARGs detected by metagenomics in either influent or secondary effluent resulted in 34 total ARGs (i.e., several ARGs were most abundant in both categories). There was an increase in 26 of the 34 ARGs in all or certain sampling events

(Figure 2-3). The relative abundance of *sul*1 increased in six sampling events excluding April 2018 and August 2018, in which the relative abundance decreased. Likewise, the relative abundance of *sul*2 increased in six sampling events, excluding February 2018 and April 2018, in which the relative abundance decreased. Notably, the calculated absolute abundances of *sul*1 and *sul*2 were perfectly correlated ($R = 1.00$, $p < 0.001$). February 2018 represents the sampling event with the greatest number of ARGs exhibiting an increase in relative abundance from influent to secondary effluent (Figure 2-3).

Table 2-3. ARGs detected in the influent only, effluent only, or shared between influent and effluent.

Sampling Event (total ARGs in influent/effluent)	# of unique ARGs detected in the influent (% total ARGs in influent)	# of unique ARGs detected in the effluent (% total ARGs in effluent)	# of ARGs detected in influent *and* effluent (% total ARGs in influent/effluent)
July 2017 (576/271)	334 (58.0)	29 (10.7)	242 (42.0/89.3)
October 2017 (670/331)	318 (47.5)	39 (11.8)	292 (52.5/88.2)
December 2017 (596/330)	309 (51.8)	43 (13.0)	287 (49.2/87.0)
February 2018 (585/309)	298 (50.9)	22 (7.1)	287 (41.1/92.9)
April 2018 (546/326)	253 (46.3)	33 (10.1)	293 (53.7/89.9)
June 2018 (643/441)	250 (38.9)	48 (10.9)	393 (61.1/89.1)
August 2018 (551/381)	219 (39.7)	49 (12.9)	332 (60.3/87.1)
October 2018 (341/325)	109 (32.0)	93 (28.6)	232 (68.0/71.4)

Table 2-4. ARGs detected only in the effluent that were also detected in the October 2018 sampling, which yielded the highest number of unique ARG detections.

Sampling Event (# ARGs shared with October 2018 sampling)	ARGs Shared
July 2017 (8)	*bla*F, *bla*CARB-12, *bla*VIM-23, *bla*LRA-19, *bla*OXA-224, *bla*OXA-29, *dfr*B2, *vat*A
October 2017 (15)	*AAC*(6')-IIb, *bla*F, *bla*IMP-19, *bla*IMP-44, *bla*LRA-10, *bla*VIM-23, *dfr*A2d, *dfr*B2, *dfr*B6, *ole*C, *srm*B, *sul*3, *van*M, *van*XO, *vat*A
December 2017 (16)	*AAC*(3)-IIIc, *abe*S, *arr*-3, *bla*F, , *bla*IMP-19, *bla*LRA-10, *bla*LRA-19, *bla*VIM-23, *dfr*A15, *dfr*B2, *dfr*B6, *mfp*A, *ole*C, *tlr*C, *vat*A, *mur*A in *Chlamydia trachomatis*
February 2018 (8)	*bla*F, *bla*IMP-19, *bla*LRA-19, *bla*VIM-2, *bla*VIM-23, *fos*A7, *tet*(Y), *van*M
April 2018 (17)	*AAC*(6')-IIb, *bla*F, *bla*FEZ-1, *bla*LRA-10, *bla*LRA-19, *bla*OXA-29, *bla*VIM-2, *bla*VIM-23, *dfr*A16, *dfr*B2, *dfr*B6, *iri*, *ole*B, *ole*C, *qnr*B72, *vat*I, *mur*A in *Chlamydia trachomatis*
June 2018 (11)	*AAC*(3)-IIIc, *bla*FEZ-1, *bla*IMP-19, *bla*LRA-10, *bla*OXA-29, *bla*VIM-2, *bla*VIM-23, *dfr*A2d, *dfr*B6, *ole*B, *sul*3
August 2018 (10)	*arr*-2, *arr*-3, *arr*-5, *bla*LRA-10, *dfr*B6, *ole*C, *qep*A, *qep*A3, *sul*3, *tet*B(48)

An average of approximately half (41.1-68.0%) of the ARGs that enter the WWTP in any given sampling event persisted through the secondary effluent (Table 2-3). There were only a relatively small number of ARGs that appear in the WWTP secondary effluent that were not detected in the influent. ARGs from the influent, in 7 out of 8 sampling events, account for close to 90% of the ARGs in the secondary effluent (i.e., the ARGs that were not removed by the treatment train). More specifically, within the core resistome of influent and effluent, four categories of ARGs were further specified: **(1)** completely removed (i.e., not detected in effluent),

(2) increased across all sampling events, **(3)** decreased across all sampling events, and **(4)** detected only in secondary effluent. There was an increase in 88 ARGs from influent to effluent in all or most sampling events. There were only 2 ARGs in category 1: *aph*(3')-VI (aminoglycoside) and *opr*Z (multidrug). Eleven ARGs that fell into category 2 belonging to the following classes: one beta-lactam (*bla*OXA-46), three rifamycin (*arr*-1, *rph*A, *rph*B), two tetracycline (*tap*, *tet*A(48)), four multidrug (*efp*A, *mex*N, *mtr*A, *mux*C), and one mupirocin, henceforth classified as "other" (*ile*S in bifidobacteria). Sixty-one ARGs were included in category 3 and no ARGs were only detected in the secondary effluent across all sampling events (category 4) (Supplementary Table 3). However, there was a range of 22 to 93 ARGs that appeared in the secondary effluent each sampling event. The greatest number of unique ARGs (i.e., highest diversity) that were detected in the secondary effluent but not the influent corresponded to the sampling event in October 2018. Thus, we analyzed the shared ARGs between the October 2018 sampling event and all other sampling events (Table 2-4). A substantial number of these shared ARGs encoded resistance to beta-lactams, although the overall relative abundance of this resistance class decreased with each sampling event.

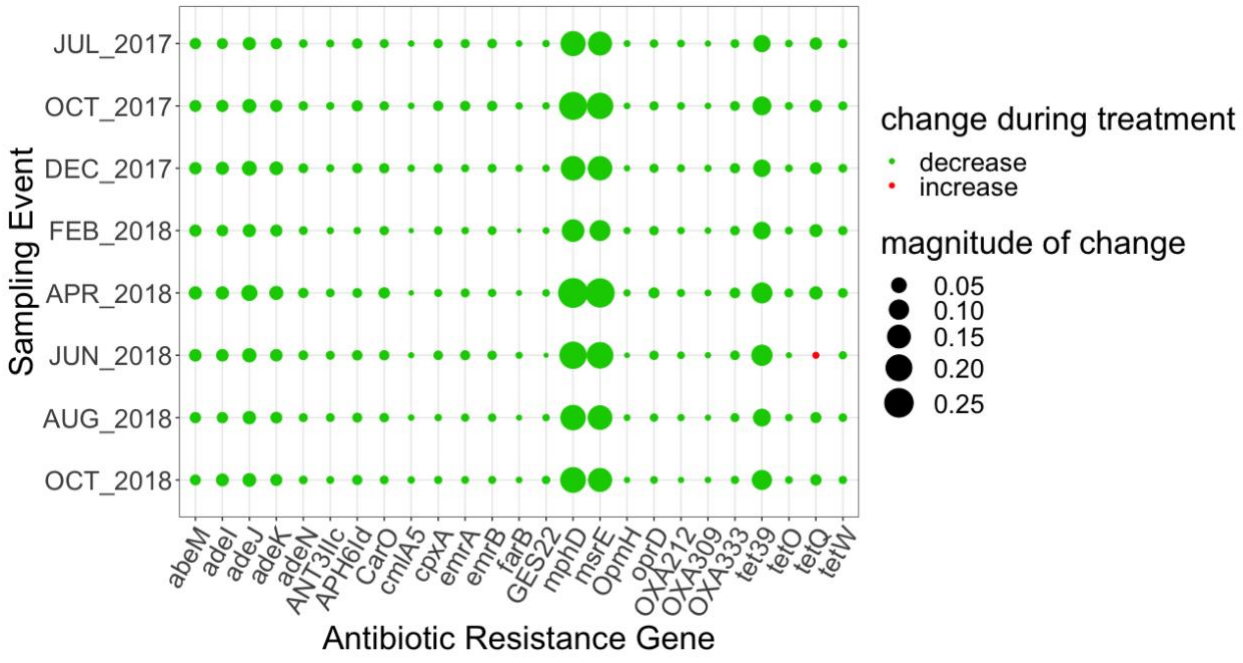

Figure 2-4. Magnitude of change in relative abundance between influent and secondary effluent of ARGs detected in the discriminatory resistome.

The 34 discriminatory ARGs were determined by ExtrARG (Gupta et al., 2019).

Discriminatory ARGs were identified via ExtrARG (Gupta et al., 2019), which employs deep learning to identify which ARGs best distinguished each treatment stage. Thirty-two ARGs were found to most effectively distinguish the influent versus the secondary effluent based on their magnitude of change in relative abundance: one aminocoumarin (*novA*), three aminoglycoside (*acr*D, *ant*(3'')-IIc, *aph*(6)-Id), ten beta-lactam (*bla*ADC-15, *car*O, *bla*FOX-10, *bla*GES-22, *opr*D in *Acinetobacter baumannii*, *bla*OXA-211, *bla*OXA-212, *bla*OXA-309, *bla*OXA-333, *bla*OXA-334), two MLS (*mph*D, *msr*E), seven tetracycline (*ade*A, *tet*32, *tet*39, *tet*40, *tet*O, *tet*Q, *tet*W), eight multidrug (abeM, *ade*I, *ade*J, *ade*K, *ade*N, *emr*A, *emr*B), and *far*B, conferring resistance to antibacterial free fatty acids (other) (Figure 2-4). All of the aforementioned ARGs decreased in relative abundance from influent to effluent in each sampling event, except *tet*Q in the June 2018 sampling event. *mph*D and *msr*E, underwent the greatest change in relative abundance between influent and effluent.

A Spearman rank order correlation analysis was performed to explore the relationship between ARG abundance as determined by qPCR and the calculated absolute abundance of ARGs by metagenomics. Log absolute abundance values of ARGs quantified via qPCR are presented in Supplementary Figure 1. Significant correlations were observed for *erm*B ($R = 0.87$, Bonferroni-corrected $p < 0.001$), aggregate *bla*TEM genes by metagenomics (*bla*TEM-17, *bla*TEM-57, *bla*TEM-75, *bla*TEM-91, *bla*TEM-166, *bla*TEM-176, *bla*TEM-194, *bla*TEM-195, *bla*TEM-207, *bla*TEM-215) and *bla*TEM by qPCR ($R = 0.84$, Bonferroni-corrected $p < 0.001$) and *sul*1 ($R = 0.83$, Bonferroni-corrected $p < 0.001$). Vancomycin resistance gene, *van*A, was only detected in the effluent of the December 2018 sampling event by metagenomics and therefore could not be correlated to qPCR data.

Shift in Microbiome through the WWTP

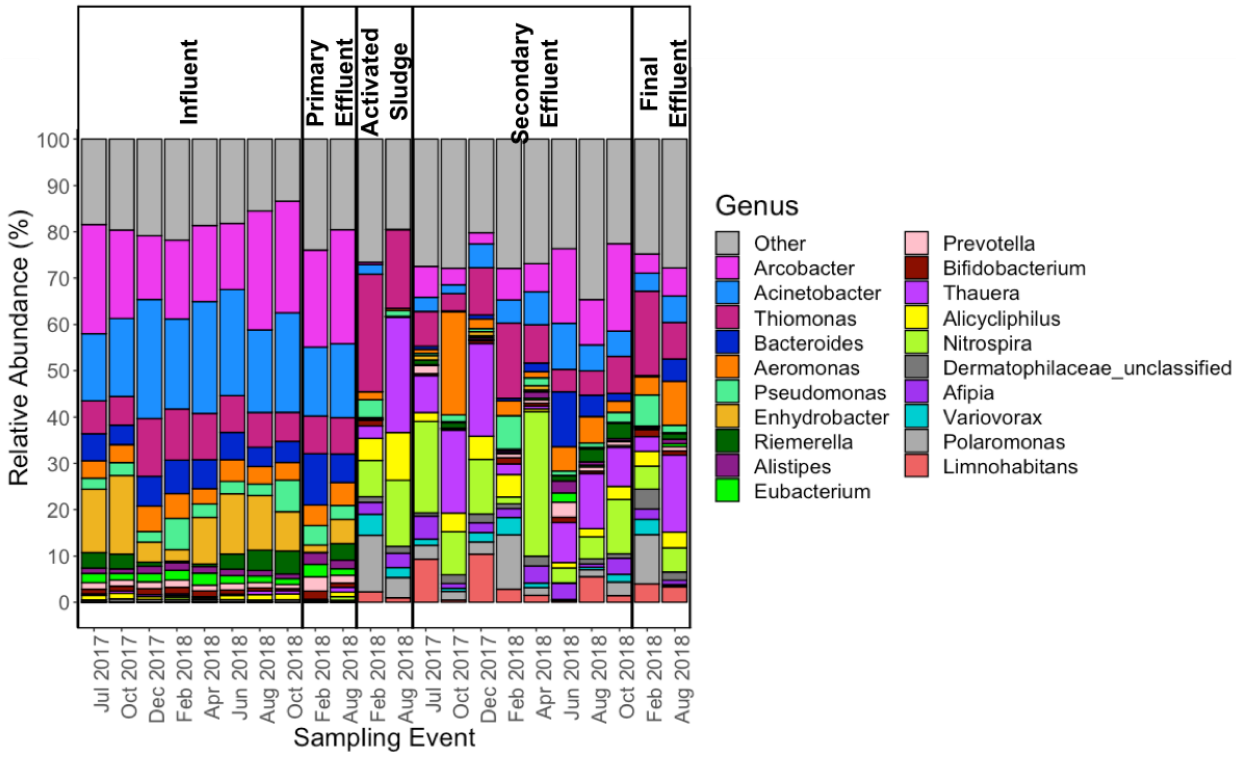

Figure 2-5. Metagenomic characterization of taxonomy in all samples.

Relative abundance of top 20 and "other" genera presented as a percentage of corresponding genetic markers quantified from metagenomic reads annotated using MetaPhlAn2 (Truong et al., 2015).

In most influent samples, *Arcobacter*, *Acinetobacter*, and *Enhydrobacter* comprised greater than 50% of the genera detected (Figure 2-5). This was not the case during the months of December 2017 and February 2018, when the presence of *Enhydrobacter* was much less than the remaining sampling events. While the influent and primary effluent were quite similar, there was a notable shift in the composition of the microbial community at the activated sludge stage. Thereafter, the composition of the secondary effluent and final effluent mirrored that of the activated sludge, suggestive that they are representative of activated sludge bacteria that escape the clarifier. Some of the more dominant genera found from activated sludge onward include *Thiomonas, Thauera,* and *Nitrospira, Polaromonas,* and *Limnohabitans*. Notably, there appears to be more variability in the abundance of the top 20 genera in activated sludge, secondary effluent, and final effluent as compared to influent and primary effluent (Figure 2-5).

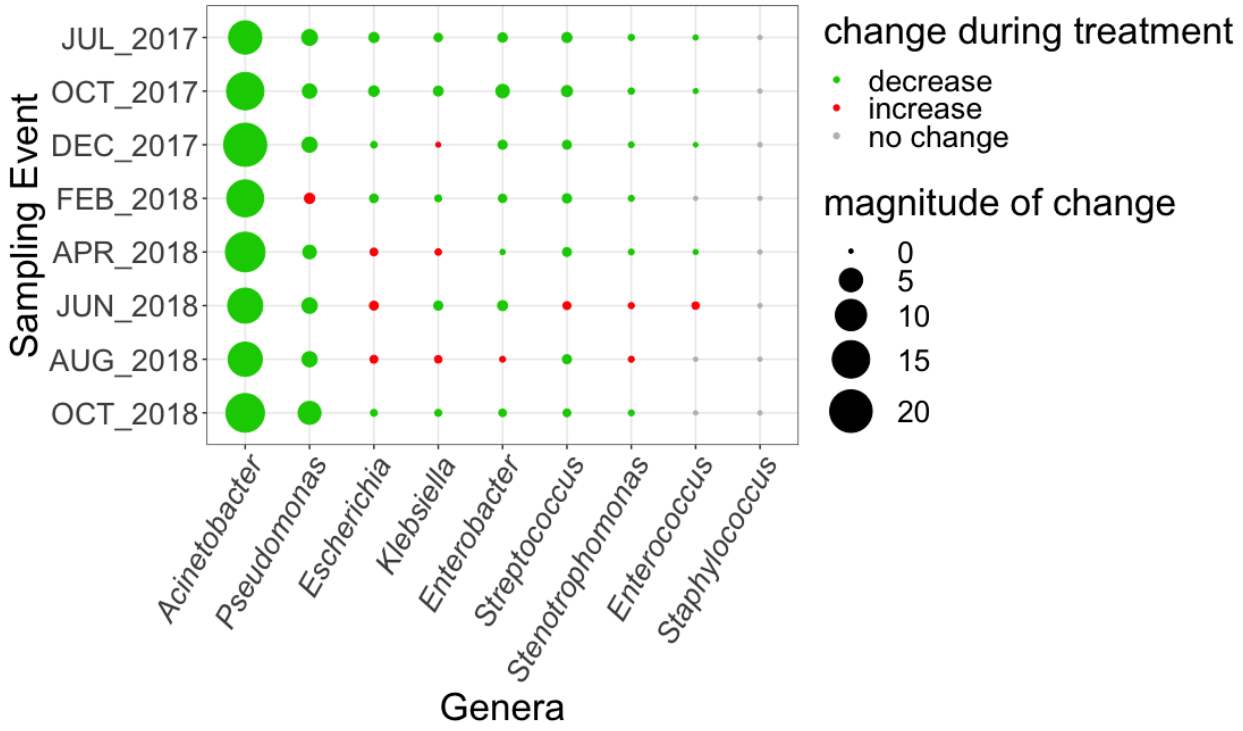

Figure 2-6. Magnitude of change between influent and secondary effluent of select pathogen-containing genera.

Relative abundance presented as a percentage of corresponding genetic markers quantified from metagenomics reads annotated using MetaPhlAn2 (Truong et al., 2015). Pathogen-containing genera of interest were selected from the 2017 Virginia state and regional cumulative antibiogram (VDH, 2017).

According to the Virginia Healthcare Emergency Management Program, the WWTP in this study is located in the Near Southwest region. Fourteen out of fifteen hospitals from this region participated in the 2017 Virginia state and regional cumulative antibiogram. Pathogens targeted in the antibiograms included: *Acinetobacter, Enterobacter, Enterococcus, Escherichia, Klebsiella, Pseudomonas, Staphylococcus, Stenotrophomonas, and Streptococcus.* As a means of linking the WWTP and local clinical data, we compared these nine genera, quantified from genetic markers in the metagenomic data using MetaPhlAn2 (Truong et al., 2015), in the influent and secondary effluent across the eight sampling events (Figure 2-6). *Enterococcus* was not detected in the influent or effluent in three sampling events or in the effluent of seven sampling events, while the relative abundance increased in the June 2018 sampling event. *Acinetobacter* exhibited a decrease in relative abundance across all sampling events. *Streptococcus* experienced a decrease in relative abundance in six sampling events, whereas it was not detected in the effluent of two sampling

events. In five sampling events, *Stenotrophomonas* was not detected in the effluent, although the relative abundance increased in August 2018. *Staphylococcus* was not detected in any influent or effluent samples. In only one sampling event, *Enterobacter* (February 2018) and *Escherichia* (October 2017) were not detected in the effluent, whereas the relative abundance of *Enterobacter* increased in one sampling event (August 2018) and the relative abundance of *Escherichia* increased in three sampling events (April 2018, June 2018, August 2018) from influent to secondary effluent. *Klebsiella* and *Pseudomonas* were detected in the influent and effluent of each sampling event, with *Klebsiella* increasing in relative abundance in three sampling events (December 2019, April 2018, August 2018) and *Pseudomonas* increasing in one sampling event (February 2018). Other than the instances previously specified, the relative abundances of the remaining pathogen-containing genera decreased across all sampling events.

Relationship between the resistome and the microbiome

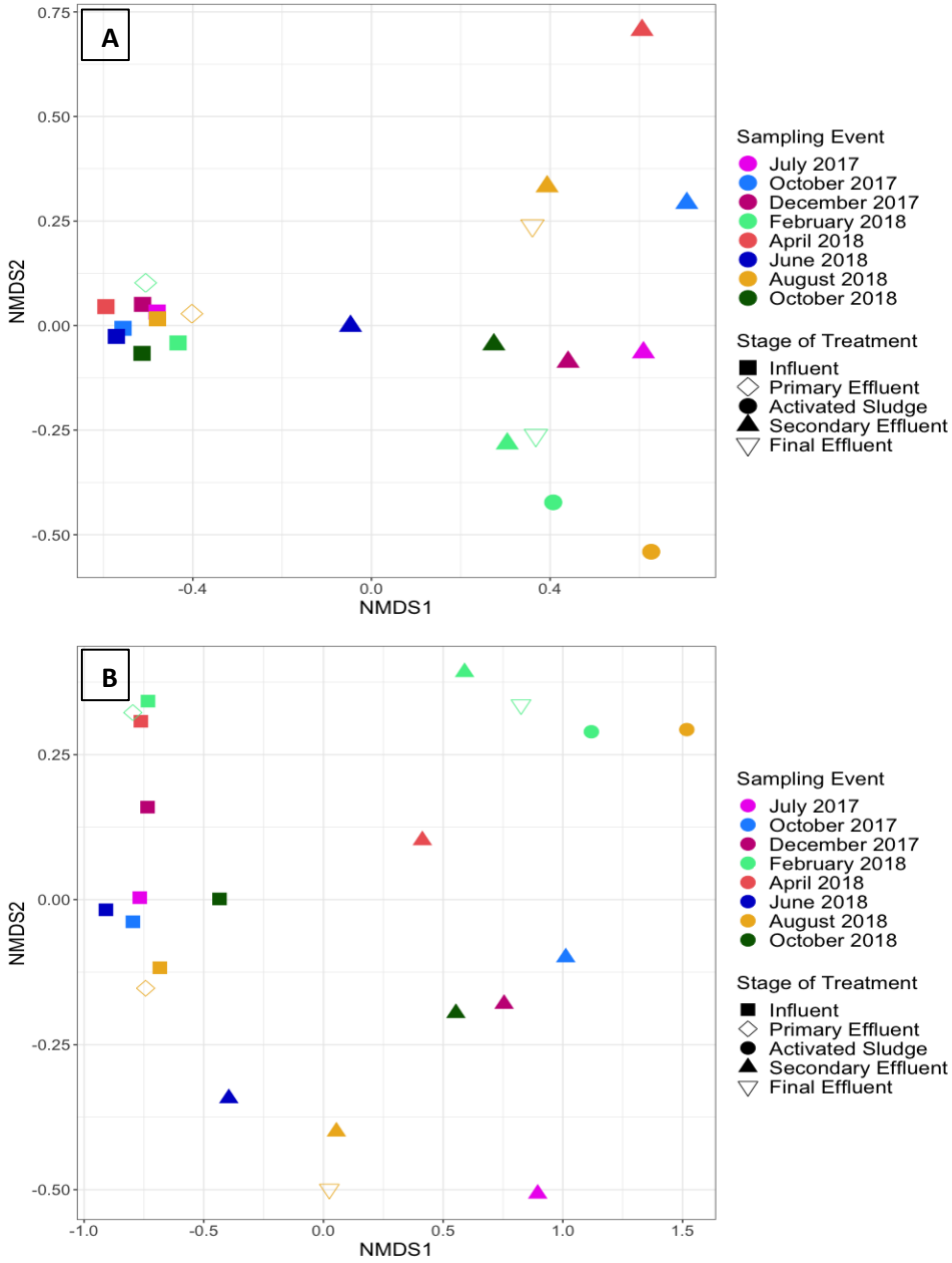

Figure 2-7. NMDS analysis of ARG profiles (ANOSIM; *R* = 0.708, *p* = 0.001) (A) and taxonomic profiles (ANOSIM; *R* = 0.6547, *p* = 0.001) (B) across all stages of treatment and sampling dates assessed by metagenomic sequencing.

Influent samples were separated from activated sludge (ANOSIM; $R = 1$, $p = 0.022$), secondary effluent (ANOSIM; $R = 0.933$, $p = 0.001$), and final effluent (ANOSIM; $R = 1$, $p = 0.022$), but not from primary effluent (ANOSIM; $R = 0.228$, $p = 0.178$). Secondary and final effluent samples were not separated (ANOSIM; $R = -0.306$, $p = 0.911$). ARGs were annotated via CARD (Jia et al., 2017) and the microbiome was annotated via MetaPhlAn2 (Truong et al., 2015).

NMDS analysis of total ARG relative abundance indicated distinct resistomes associated with each stage of treatment (ANOSIM; #ARGs = 953, $R = 0.708$, $p = 0.001$; Figure 2-7). Influent samples were separated from activated sludge (ANOSIM; #ARGs = 953, $R = 1$, $p = 0.022$), secondary effluent (ANOSIM; #ARGs = 953, $R = 0.933$, $p = 0.001$), and final effluent (ANOSIM; #ARGs = 953, $R = 1$, $p = 0.022$), but not from primary effluent (ANOSIM; #ARGs = 953, $R = 0.228$, $p = 0.178$). Activated sludge samples were not separated from secondary effluent (ANOSIM; #ARGs = 953, $R = 0.151$, $p = 0.267$) or final effluent (ANOSIM; #ARGs = 953, $R = 0.25$, $p = 0.333$). The ANOSIM R statistic and significance level of each pairwise test between each stage of treatment based on relative abundance is available in Supplementary Table 4. ARGs that were not detected across all samples in a subset were excluded from ANOSIM analysis.

Taxonomic profiles at the genus level followed a similar trend as ARGs and were also uniquely separated by stage of treatment (ANOSIM; $R = 0.6547$, $p = 0.001$). Influent samples were separated from activated sludge (ANOSIM; $R = 1$, $p = 0.019$), secondary effluent (ANOSIM; $R = 0.801$, $p = 0.002$), and final effluent (ANOSIM; $R = 1$, $p = 0.024$), but not from primary effluent (ANOSIM; $R = 0.31$, $p = 0.136$). Activated sludge samples were not separated from secondary effluent (ANOSIM; $R = 0.289$, $p = 0.15$) or final effluent (ANOSIM; $R = 0.25$, $p = 0.667$).The ANOSIM R statistic and significance level of each pairwise test between each stage of treatment based on genus level relative abundance is available in Supplementary Table 5. A Procrustes analysis was performed on the ARG and taxonomic NMDSs of all 22 samples, assuming symmetry, resulting in a Procrustes Sum of Squares value equal to 0.261 ($p = 0.001$). This relatively low value suggests that ARG and taxonomic profiles behave similarly across the WWTP with time.

Temporal variability

Table 2-5. Coefficient of variation, as percent (%), in influent and secondary effluent

Antibiotic Resistance Class	Influent (n^a=8)	Secondary Effluent (n^a=8)
Total ARG relative abundance	9.1	30
aminocoumarin	24	91
aminoglycoside	16	43
beta-lactam	8.7	54

elfamycin	ND[b]	NA[c]
fosfomycin	22	66
glycopeptide	25	67
MLS	15	42
peptide	15	40
phenicol	12	63
quinolone	19	60
rifamycin	41	48
sulfonamide	21	45
tetracycline	12	58
trimethoprim	20	77
multidrug	11	30
other	20	34

[a]n = number of samples.
[b]ARGs conferring resistance to this antibiotic class not detected in any samples.
[c]ARGs conferring resistance to this antibiotic class detected in only one sample.

According to the coefficients of variation, as percent, of the total ARG relative abundance of influent (9.1%) versus secondary effluent (30%) samples, it appears that influent exhibited less variability in the resistome with time than the secondary effluent (Table 2-5). Influent samples were consistently less variable than secondary effluent samples across all antibiotic resistance classes. Variability ranged from: 8.7-41% in the influent and from 30-91% in secondary effluent (Table 2-5).

Influent samples did not exhibit distinct separation based on relative abundance of ARGs when grouped by season (ANOSIM; #ARGS = 859, $R = 0.1458$, $p = 0.241$; Supplementary Figure 2) or grouped seasons (ANOSIM; #ARGS = 859, $R = 0.2396$, $p = 0.064$; Supplementary Figure 3). Abundance of genera also did not exhibit distinct separation based on grouped seasons (ANOSIM; $R = 0.1354$, $p = 0.213$; Supplementary Figure 5). However, by season, more distinct separation of the taxonomic profile was observed (ANOSIM; $R = 0.5208$, $p = 0.04$; Supplementary Figure 4). Similar trends were observed based on relative abundances of secondary effluent samples, the results were as follows: ARG profiles grouped by season (ANOSIM; #ARGS = 637, $R = -0.1667$, $p = 0.785$; Supplementary Figure 2), ARG profiles based on grouped seasons

(ANOSIM; #ARGS = 637, R = -0.04167, p = 0.63; Supplementary Figure 3), taxonomic profiles grouped by season (ANOSIM; R = -0.1458, p = 0.775; Supplementary Figure 4), and taxonomic profiles based on grouped seasons (ANOSIM; R = -0.1146, p = 0.789; Supplementary Figure 5) did not exhibit distinct separation.

Relative Resistome Risk

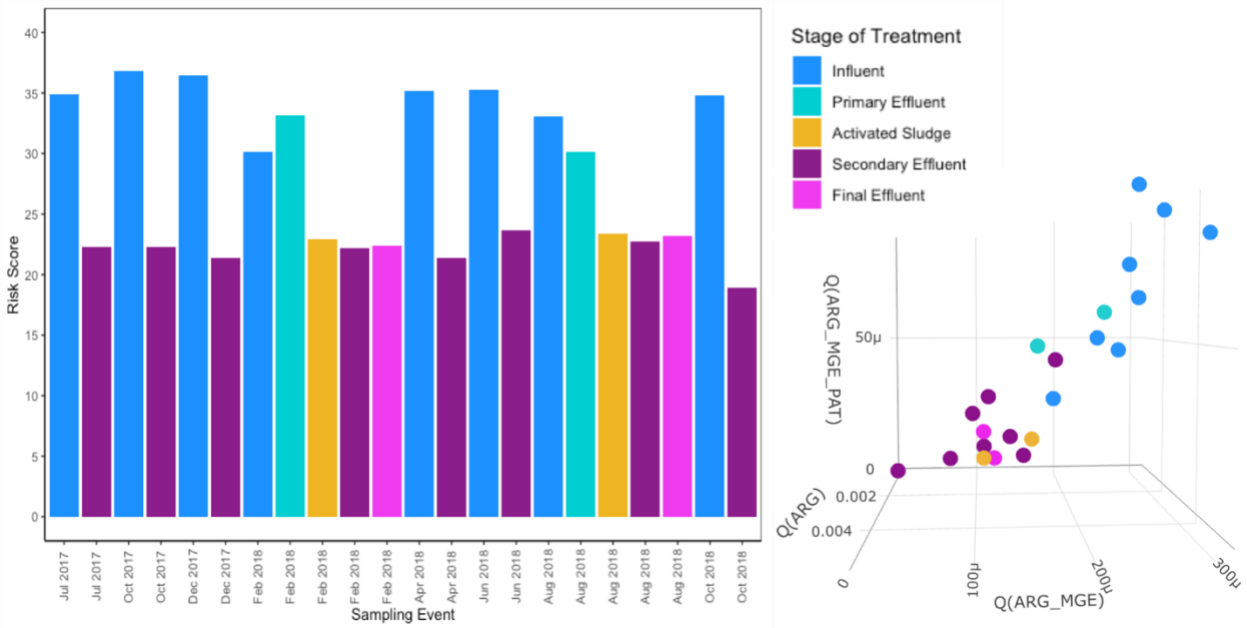

Figure 2-8. Relative resistome risk scores and projection in 3D hazard space for each sample.

Risk scores and 3D hazard space values determined by MetaCompare (Oh et al., 2018).

MetaCompare (Oh et al., 2018) assigns relative resistome risk scores based on the distance each sample point is from an established theoretical, maximum risk hazard score in a 3-dimensional "hazard space." A sample's point is this 3-dimensional space is determined as: (1) the number of occurrences of ARGs on assembled contigs normalized to the total number of contigs in a given sample, (2) the number of co-occurrences of ARGs and MGEs normalized to the total number of contigs, and (3) the number of co-occurrences of ARGs, MGEs, and human-like pathogens normalized to the total number of contigs. As would be expected based on the WWTP achieving its intended purpose of reducing pathogens, MetaCompare indicated that there was a higher resistome risk associated with influent and primary effluent samples than activated sludge, secondary effluent, and final effluent (Figure 2-8). There was a significant difference between

relative resistome risk scores calculated from the influent samples compared to secondary effluent (Wilcoxon, paired; p = 0.007813). The data used to establish relative resistome risk in MetaCompare can be found in Supplementary Table 6.

It is noted that MetaCompare analysis requires assembly of the metagenomic data. Details of *de novo* assembly can be found in Supplementary Table 6. In this study, the percent of sequences successfully assembled across samples ranged from 24-69% and was significantly different among sample types (Kruskal-Wallis, p = 0.0229), as higher percentage assembly was observed in most secondary effluent samples. However, the high rate (i.e., only four samples with <40% assembled) and consistency of assembly across sample types increases confidence in the resistome risk analysis (Supplementary Table 6).

ARGs of potential local, clinical relevance

A database of 931 ARGs known in clinical isolates was compiled. Eleven clinically-relevant ARGs (Supplementary Table 7) detected were also detected in the core resistome across all samples. Within the discriminatory resistome of the influent and secondary effluent, there were 4 clinically-relevant ARGs (Supplementary Table 7) detected. Notably, 189 of the 954 total ARGs detected across all samples were also found in the database of clinically-relevant ARGs.

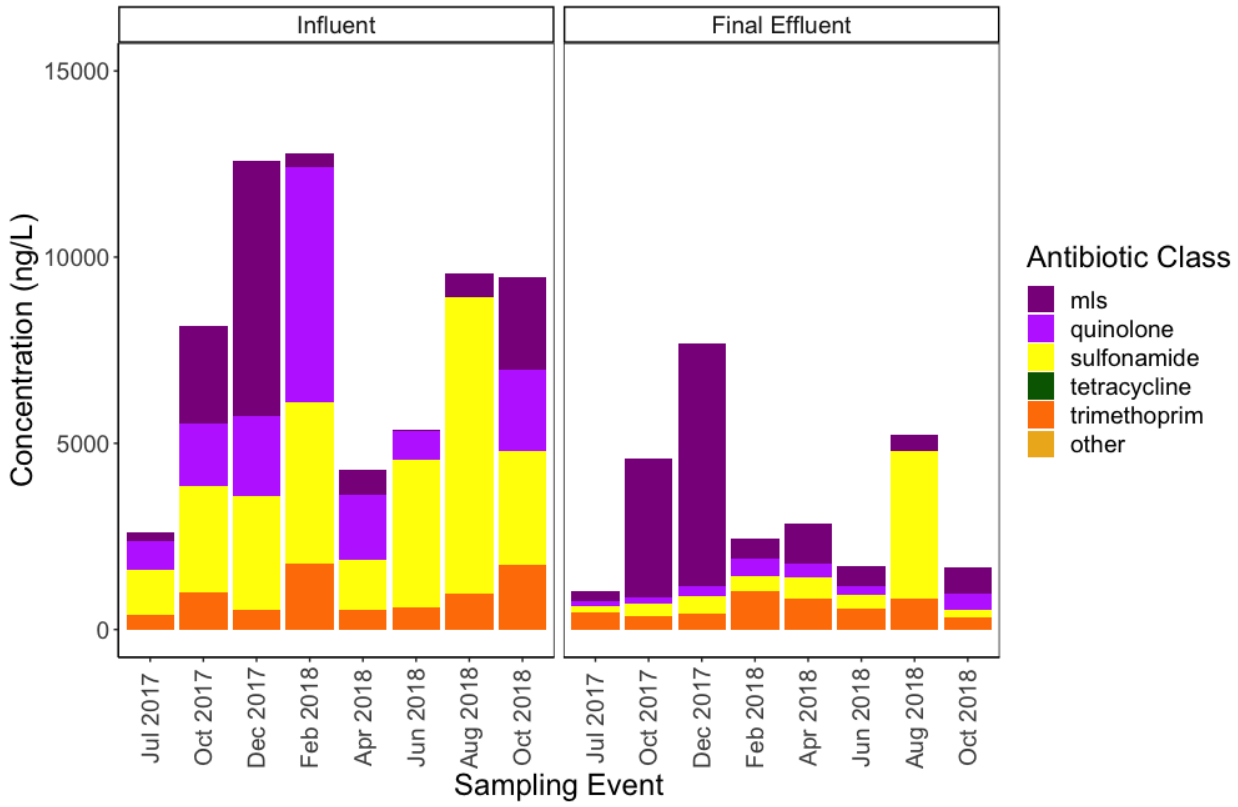

Figure 2-9. Measurements of antibiotics in influent and final effluent samples grouped by resistance class.

Concentration (ng/L) of antibiotics detected via ultraperformance liquid chromatography-tandem mass spectrometry as described previously (Singh et al., 2019).

Antibiotic Analysis

Analysis of antibiotics grouped by resistance class in samples taken indicated a similar pattern as ARGs, with a tendency to reduce from the influent to the final effluent (Figure 2-9). Concentrations of each antibiotic detected are reported in Supplementary Table 8. However, among the antibiotics tested, the MLS and trimethoprim antibiotics appeared to be the most persistent and difficult to remove. Total antibiotic loading in the influent ranged between 2,614 and 12,780 ng/L, while final effluent ranged between 1,045 and 7,665 ng/L. The highest antibiotic loading in the influent occurred in the month of February 2018 (12,780 ng/L), closely followed by December 2017 (12,584 ng/L). The highest antibiotic loading in the final effluent occurred in the month of December 2017 (7,665 ng/L), corresponding to a removal efficiency of approximately

39%. Total antibiotic concentration between the two stages of treatment were significantly different (Wilcoxon, paired; $p = 0.0078$).

Sulfamethoxazole and acetylsulfamethoxazole were the only sulfonamides detected in the influent and effluent samples, however the concentration of sulfamethoxazole was never greater than the proposed no effect concentration (PNEC) (Bengtsson-Palme & Larson, 2016) below which no selection of antibiotic resistance bacteria is anticipated (Supplementary Table 8). The concentration of acetylsulfamethoxazole was greater than sulfamethoxazole in all sampling events, except August 2018, and the two were not strongly correlated ($R = 0.1557$, $p = 0.7128$). Both compounds were weakly correlated with core ARGs *sul*1 (sulfamethoxazole, $R = 0.18$; acetylsulfamethoxazole, $R = 0.24$) and *sul*2 (sulfamethoxazole, $R = 0.18$; acetylsulfamethoxazole, $R = 0.24$). Aggregate sulfonaminde antibiotics and sulfonamide ARGs were not correlated ($R = 0.14$, $p = 0.7358$). Sulfonamides and trimethoprim antibiotics showed a relatively strong correlation in the influent ($R = 0.67$, $p = 0.0710$). Of the ARGs detected within the trimethoprim resistant dihydrofolate reductase (dfr) gene family, only 2 ARGs exhibited a correlation coefficient $R > 0.5$ in the influent: *dfr*A17 ($R = 0.68$, $p = 0.0618$) and *dfr*A19 ($R = 0.85$, $p = 0.0082$). Trimethoprim and associated resistance genes were not strongly correlated ($R = 0.29$, $p = 0.4927$). While the concentration of sulfamethoxazole did not exceed the PNEC value in any influent samples, trimethoprim exceeded the PNEC in 7 out of 8 sampling events (Supplementary Table 8).

Of the MLS antibiotics, azithromycin was the most persistent MLS antibiotic from influent to final effluent, positively correlating with *erm*35 ($R = 0.82$, $p = 0.0114$), *erm*F ($R = 0.80$, $p = 0.0165$), *erm*G ($R = 0.72$, $p = 0.0446$), *mex*A ($R = 0.82$, $p = 0.0114$), *mex*B ($R = 0.80$, $p = 0.0165$), *mph*A ($R = 0.82$, $p = 0.0114$), *mtr*A ($R = 0.80$, $p = 0.0165$), *mtr*C ($R = 0.90$, $p = 0.0024$), *mtr*D ($R = 0.87$, $p = 0.0045$), *mtr*E ($R = 0.83$, $p = 0.0114$), and *mtr*R ($R = 0.72$, $p = 0.0446$). However, clarithromycin exhibits strong negative correlations with *erm*38 ($R = -0.75$, $p = 0.0326$), *erm*39 ($R = -0.77$, $p = 0.0244$), *mtr*C ($R = -0.83$, $p = 0.0109$), *mtr*D ($R = -0.71$, $p = 0.0500$), *mtr*E ($R = -0.76$, $p = 0.0299$), and *mtr*R ($R = -0.95$, $p = 0.0003$). Furthermore, azithromycin and clarithromycin appeared to be negatively correlated ($R = -0.69$, $p = 0.0597$). In 5 out of 8 sampling events, azithromycin or clarithromycin were not detected simultaneously. Anhydro erythromycin and respective MLS ARGs did not correlate, while erythromycin was not detected. Aggregate values of MLS ARGs and MLS antibiotics were not strongly correlated ($R = 0.52$, $p = 0.1827$).

There were no strong correlations with ciprofloxacin in the influent, the only quinolone antibiotic detected of those screened, nor were there any strong correlations with aggregate quinolone ARG abundance. (R = 0.17, p = 0.6932). Although, the concentration of ciprofloxacin exceeded the PNEC in all sampling events in which it was detected (Supplementary Table 8).

Sulfamethoxazole/trimethoprim, ciprofloxacin, and erythromycin resistances were tested in the 2017 Virginia state and regional cumulative antibiogram. Thirty-six percent of 239 *Acinetobacter baumannii* complex isolates from 5 facilities, 15% of 454 *Enterobacter cloacae* isolates from 5 facilities, 23% of 23,761 *Escherichia coli* isolates from 13 facilities, 11% of 3,759 *Klebsiella pneumoniae* isolates from 13 facilities, and 4% of 7,455 *Staphylococcus aureus* isolates from 10 facilities conferred resistance to sulfamethoxazole/trimethoprim. Thirty-three percent of 151 *Acinetobacter baumannii* complex isolates from 3 facilities, 11% of 442 *Enterobacter cloacae* isolates from 4 facilities, 23% of 23,387 *Escherichia coli* isolates from 10 facilities, 5% of 3,274 *Klebsiella pneumoniae* isolates from 10 facilities, and 18% of 2,245 *Pseudomonas aeruginosa* isolates from 8 facilities conferred resistance to ciprofloxacin. 64% of 7,692 *Staphylococcus aureus* isolates from 11 facilities, 46% of 232 *Streptococcus pneumoniae* isolates from 4 facilities, and 65% of 122 *Streptococcus agalactiae* isolates from 2 facilities conferred resistance to erythromycin. However, erythromycin was not detected in any influent or final effluent samples (Supplementary Table 8).

Wastewater physiochemical parameters

Correlations were examined between several wastewater physiochemical parameters measured at the time of sampling or monitored by the WWTP (e.g., daily TSS measurements, Supplementary Table 1. Influent water temperature, ambient temperature, DO, pH, and TSS were strongly, positively correlated (R > 0.7) with 11, 5, 19, 20, and 17 ARGs, respectively. Whereas, Influent water temperature, ambient temperature, DO, pH, and TSS were strongly, negatively correlated (R < 0.7) with 17, 7, 37, 18, and 1 ARGs, respectively.

Discussion

This study provides high resolution insight into the composition and variance of the antibiotic resistome over time at a small (~3MGD) conventional WWTP. In particular, the repeated sampling through various stages of treatment, along with core and discriminatory ARG analysis,

enabled assessment of which ARGs are most effectively removed and which persist in the effluent. Further, comparison with antibiotic removal data and local clinical resistance served to link the observed patterns in ARG composition and genera containing pathogens with antibiotic use and documented types and forms of resistant pathogens causing infections in the community. Overall, repeated sampling through multiple stages of treatment enabled assessment of treatment efficacy and identification of indicator ARGs and other metagenomic-derived metrics that monitoring of the influent and effluent can provide suitable targets for antibiotic resistance surveillance of WWTPs.

From influent to secondary effluent, ~50% reduction in total ARG relative abundance was observed, along with a distinct shift in the resistome composition. Approximately the same reduction percentage was observed in a previous study, which was largely attributed to the decrease in 16S rRNA genes (i.e., the removal of total bacteria) (Bengtsson-Palme et al., 2016). Additionally, there was a 2-3 log removal of 16S rRNA by qPCR and the sum of each resistance class detected by metagenomics based on calculated absolute abundance. Gao et al. (2012) observed a 2-3 log removal of ARGs quantified by qPCR. The number of ARGs detected across all sampling events decreased from 859 in the influent to 637 in the secondary effluent. Lira et al. (2020) also observed a decrease in individual ARGs from influent to final effluent (post-UV disinfection), although only 259 ARGs were detected overall. Multidrug ARGs were the most persistent, accounting for up to 40% of total ARG relative abundance by the secondary effluent, while the most substantial reduction occurred in the MLS resistance class. Aminocoumarin, glycopeptide, phenicol, rifamycin, sulfonamide, trimethoprim, and other resistance classes experienced an overall increase in ARG relative abundance in at least four sampling events. February 2018 exhibited the greatest number of individual core ARGs which increased from influent to effluent, while June 2018 accounted for the least removal of total ARG relative abundance. The discriminatory resistome was comprised of ARGs that most effectively distinguished the influent from secondary effluent using the randomized tree algorithm employed by ExtrARG (Gupta et al., 2019). It should be noted that this list of discriminatory ARGs is not necessarily reflective of presence/absence of ARG detection in the influent versus secondary effluent. Therefore, there were several most abundant core ARGs that appeared in the discriminatory resistome due to the magnitude of change in relative abundance from influent to secondary effluent. These shared ARGs included: *mph*D, *msr*E, *tet*39, *tet*Q, *ade*J, *ade*K, of which

all but *tet*Q decreased in relative abundance during each sampling event (the relative abundance of *tet*Q increased in June 2018). In a study of a global transect of WWTP influent core resistomes spanning three continents, *mph*D, *msr*E, *tet*Q, and *ade*J were also identified among the top 25 most abundant ARGs in influent samples (Riquelme et al., in preparation).

The relatively tight clustering of influent samples, visualized by NMDS analysis, suggests that the incoming resistome is relatively stable year-round among sampling events. Greater variability is observed in the resistome of the secondary effluent with repeat sampling compared to the influent, further indicated by the COV values of each antibiotic resistance class. The influent does appear to influence the composition of the effluent from a presence/absence viewpoint, based on the occurrence of approximately 90% of secondary effluent ARGs also having been detected in the influent. This finding is important in that it suggests that it does matter what goes down the drain and that the activated sludge barrier does not completely erase the influence of the influent resistome on that of the effluent resistome. This suggests that policies aimed at restricting what is discharged to WWTPs could in fact influence input of ARGs to receiving environments.

There did not appear to be distinct grouping of influent resistomes by season (winter, spring, summer, fall) or grouped seasons (winter/spring, summer/fall) based on ARG profiles. This finding is consistent with no observed seasonality in the monthly sampling of the activated sludge at a Hong Kong WWTP over 9 years, although the authors hypothesized that this was due to minimal local shifts in temperature (Yin et al., 2019). The distinct separation of influent from activated sludge, secondary effluent, and final effluent in the NMDS plots suggests a relatively stable resistome in the influent that subsequently shifts during activated sludge. While the resistome composition of activated sludge was relatively stable in this study, it was noted that the activated sludge resistome shifted in composition every two to three years at a WWTP in Hong Kong, a turnover period that would not have been captured over the duration of the present study (Yin et al., 2019). Interestingly, the effluent resistome was generally more variable over the sampling period than the influent resistome. This is opposite of the expectation that activated sludge produces a stable ecological environment that essentially "buffers" the effects of variation observed in the influent (Dai et al., in review). Overall, the findings suggest that performance of wastewater treatment can vary with time in terms of ability to attenuate ARGs and therefore targeted surveillance of effluents is warranted. While the microbiome was also separated based on stage of treatment, it did not appear that it was as stable as the resistome throughout the 18-

month sampling period. June 2018 and August 2018 represented the sampling events with the most occurrences of increased abundance of pathogen-containing genera of local clincal-importance (4 out of 9 genera).

An average removal of approximately 40-50% was observed for both total antibiotic load and total ARG relative abundance. Only two out of ten sulfonamides were detected; neither *sul*1 nor *sul*2 correlated with these sulfonamides in the influent. This finding was contrary to the results of a study conducted showing a strong correlation between *sul*1 and total sulfonamide concentration (majority sulfamethoxazole) in a conventional, municipal WWTP (Gao et al., 2012). While sulfonamides were largely removed between influent and final effluent and the absolute abundance of *sul*1 by qPCR, there was an increase in relative abundance in six sampling events for both *sul*1 and *sul*2. Sulfamethoxazole is often prescribed in addition to trimethoprim (Bushby, 1975); acetylsulfamethoxazole is a transformation product of sulfamethoxazole. This could explain the relatively strong correlation between acetylsulfamethoxazole and trimethoprim in the influent, with acetylsulfamethoxazole being more abundant than sulfamethoxazole. The abundance of trimethoprim was not indicative of the abundance of corresponding ARGs in the influent. Furthermore, the abundance of trimethoprim and its aggregate ARGs abundance followed opposite trends in 7 out of 8 sampling events. Ciprofloxacin, the only one of six quinolone antibiotics detected, was effectively removed through the WWTP, as was the relative abundance of quinolone ARGs. However, ciprofloxacin and its respective ARGs were not strongly correlated in the influent. MLS antibiotics, especially azithromycin, were the most persistent among the measured antibiotic classes, most often increasing in concentration from influent to final effluent and appearing in the effluent although not detected in the influent. Whereas there was a consistent decrease in the relative abundance of MLS ARGs between influent and secondary effluent according to shotgun metagenomic sequencing, the overall load of the MLS class of ARGs substantially decreased from influent to effluent. Of the ARGs positively correlating with azithromycin, *erm*F, *mex*B, *mph*A, *mtr*A, and *mtr*D were represented in the core resistome, *erm*F was one of the top 25 most abundant ARGs in the influent, while *mtr*A was one of the top 25 most abundant ARGs in the effluent and classified as category 2. Overall, these results suggest that, while there may be potential selective pressure of certain antibiotics on ARGs in the influent, ultimately the fate of antibiotics did not correspond well with the fate of respective ARGs. In most cases, antibiotic concentrations greater than the PNEC were not indicative of significant ARG

correlations (e.g., the concentration of ciprofloxacin was greater than the PNEC in seven sampling events, yet no significant correlations with ARGs were observed). Other studies have similarly noted lack of correlations between antibiotic residues and ARG abundance (Bengtsson-Palme et al., 2016; Parnanen et al., 2019; Hendriksen et al., 2019; Riquelme et al., in preparation). One limitation of the current study is the inability to detect antibiotics of several highly abundant resistance classes (e.g., beta-lactams, tetracyclines), especially as beta-lactam ARGs accounted for a large portion of the discriminatory resistome and category 4 ARGs. However, beta-lactams degrade rapidly under environmental conditions and few studies have reported their detection in WWTPs (Singh et al., 2019).

In the February 2018 and August 2018 sampling events, the greatest total ARG relative abundance removal occurred between the activated sludge and secondary effluent samples. It is likely that the biological processes within the activated sludge compartment shift the composition of the resistome, while the settling process in secondary clarification causes a reduction in total ARG relative abundance and total antibiotic load (Yuan et al., 2016).

Based on this study, several recommendations can be made with respect to surveillance of antibiotic resistance in WWTPs. In general, the influent can be monitored to provide information about changing patterns of antibiotic use and resistant pathogens in a given community with time (Aarestrup & Woolhouse, 2020), but also as an indicator of clinically-important ARGs that could potentially escape into the effluent. Further, secondary effluent is also worthy of targeting given that it is variable with time and several ARGs of clinical concern were found there. While secondary effluent is often disinfected before discharge, we recommend sampling before disinfectant given that this will yield more DNA for the analysis and that the resistomes were indistinguishable. The secondary effluent also represents the worst case of what could be discharged to receiving environments or be subject to reuse.

Metagenomics was found to yield rich information about resistomes and associated microbiomes that could be mined to address various questions and identify suitable monitoring targets. Strong correlations between ARGs measured by qPCR is an encouraging indication that shotgun metagenomic sequencing yields quantitative information. In terms of metrics, both core and discriminatory resistome analysis revealed several ARGs of clinical concern that are worthy of incorporating into future monitoring efforts. In particular, MetaCompare analysis provided a comprehensive metric for assessing the relative risk of effluents in terms of the potential for ARGs

to be mobile and carried in pathogens. Consistent with reduction of pathogens, resistome risk scores consistently decreased from influent to effluent, as would be expected. The findings here can help inform approaches for surveillance of antibiotic resistance in WWTPs, targeting locations, frequencies, and metrics that are informative locally and comparative globally.

Conclusions

The overlap between the ARGs in the core resistome, discriminatory resistome, those belonging to the four categories presents candidate ARGs that can be further monitored at a given WWTP following a short-term metagenomic sampling campaign. The strong correlation between the genes detected via qPCR and those annotated via metagenomic sequencing puts forth promising technologies for long-term, local and global WWTP monitoring.

Acknowledgements

We would like to thank the WWTP for their participation in our study and multiple sampling teams from Virginia Tech. We also thank the Advanced Research Center (ARC) of Virginia Tech for technical support. We are truly grateful to our colleagues who aided in sampling the WWTP: Jose Garcia, Ayella Maile-Moskowitz, M. Storme Spencer, Mariah Gnegy, and Kris Mapili. This study is supported by National Science Foundation (NSF) OISE award (#1545756), ECCSS NNCI award (#1542100), CSSI award (#2004751), and Center for Science and Engineering of the Exposome at the Virginia Tech Institute for Critical Technology and Applied Science (ICTAS).

References

Aarestrup, F. M. & Woolhouse, M. E. J. Using sewage for surveillance of antimicrobial resistance. *Science* 367, 630-632, doi:10.1126/science.aba3432 **(2020)**.

Arango-Argoty, G., Singh, G., Heath, L. S., Pruden, A., Xiao, W., & Zhang, L. MetaStorm: a public resource for customizable metagenomics annotation. *PLoS ONE* 11, e0162442, doi:10.1371/journal.pone.0162442 **(2016)**.

Bengtsson-Palme, J. & Larsson, D. G. Concentrations of antibiotics predicted to select for resistant bacteria: proposed limits for environmental regulation. *Environ. Int.* 86, 140-149, doi:10.1016/j.envint.2015.10.015 **(2016)**.

Bengtsson-Palme, J., et al. Elucidating selection processes for antibiotic resistance in sewage treatment plants using metagenomics. *Sci. Total Environ.* 572, 697–712, doi:10.1016/j.scitotenv.2016.06.228 **(2016)**.

Bibbal, D., Dupouy, V., Ferre, J. P., Toutain, P. L., Fayet, O., Prere, M. F., & Bousquet-Melou, A. Impact of three ampicillin dosage regimens on selection of ampicillin resistance in Enterobacteriaceae and excretion of bla(TEM) genes in swine feces. *Appl. Environ. Microbiol.* 73, 4785−4790, doi:10.1128/AEM.00252-07 **(2007)**.

Bushby, S. R. Synergy of trimethoprim-sulfamethoxazole. *Can. Med. Assoc. J.* 112, 63-66 **(1975)**.

Chen, J., Zhongtang, Y., Michel Jr., F. C., Wittum, T., & Morrison, M. Development and application of real-time PCR assays for quantification of *erm* genes conferring resistance to macrolides-lincosamides-streptogramin b in livestock manure and manure management systems. *Appl. Environ. Microbiol.* 73, 4405-4416, doi:10.1128/AEM.02799-06 **(2007)**.

Colomer-Lluch, M., Jofre, J., & Muniesa, M. Quinolone resistance genes (qnrA and qnrS) in bacteriophage particles from wastewater samples and the effect of inducing agents on packaged antibiotic resistance genes. *J. Antimicrob. Chemother.* 69, 1265−1274, doi:10.1093/jac/dkt528 **(2014)**.

Dutka-Malen, S., Evers, S., & Courvalin, P. Detection of glycopeptide resistance genotypes and identification to the species level of clinically relevant enterococci by PCR. *J. Clin. Microbiol.* 33, 24−27, doi:10.1128/JCM.33.1.24-27.1995 **(1995)**.

Gao, P., Munir, M., & Xagoraraki, I. Correlation of tetracycline and sulfonamide antibiotics with corresponding resistance genes and resistant bacteria in a conventional municipal wastewater treatment plant. *Sci. Total Environ.* 421-422, 171-173, doi:10.1016/j.scitotenv.2012.01.061 **(2012)**.

Gupta, S., Arango-Argoty, G., Zhang, L., Pruden, A., & Vikesland, P. J. Identification of discriminatory antibiotic resistance genes among environmental resistomes using extremely randomized tree algorithm. *Microbiome* 7, 123, doi:10.1186/s40168-019-0735-1 **(2019)**.

Hardwick, S. A., Stokes, H. W., Findlay, S., Taylor, M., & Gillings, M. R. Quantification of class 1 integron abundance in natural environments using real-time quantitative PCR. *FEMS Microbiol. Lett.* 278, 207−212 **(2008)**.

Hendriksen, R. S. et al. Global monitoring of antimicrobial resistance based on metagenomics analyses of urban sewage. *Nat. Commun.* 10, 1124, doi:10.1038/s41467-019-08853-3 **(2019)**.

Jia, B. et al. CARD 2017: expansion and model-centric curation of the comprehensive antibiotic resistance database. *Nucleic Acids Res.* 45, D566-D573, doi:10.1093/nar/gkw1004 **(2017)**.

Joseph, S. M., Battaglia, T., Maritz, J. M., Carlton, J. M. & Blaser, M. J. Longitudinal comparison of bacterial diversity and antibiotic resistance genes in New York City sewage. *Msystems* 4, doi:10.1128/mSystems.00327-19 **(2019)**.

Ju, F. et al. Wastewater treatment plant resistomes are shaped by bacterial composition, genetic exchange, and upregulated expression in the effluent microbiomes. *ISME J.* 13, 346-360, doi:10.1038/s41396-018-0277-8 **(2019)**.

Kim, S., Yun, Z., Ha, U. -H., Lee, S., Park, H., Kwon, E. E., Cho, Y. et al. Transfer of antibiotic resistance plasmids in pure and activated sludge cultures in the presence of environmentally representative micro-contaminant concentrations. *Sci. Total Environ.* 468–469, 813–820 doi:10.1016/j.scitotenv.2013.08.100 **(2014)**.

Kindt, R., Legendre, P., Hara, B. O., Simpson, G. L., Stevens, M. H. H., & Wagner, H. *The vegan Package*. **(2008)**.

Li, B., Yang, Y., Ma, L., Ju, F., Guo, F., Tiedje, J. M., & Zhang, T. Metagenomic and network analysis reveal wide distribution and co-occurrence of environmental antibiotic resistance genes. *ISME J.* 9, 2490–2502, doi:10.1038/ismej.2015.59 **(2015)**.

Lira, F., Vaz-Moreira, I., Tamames, J., Manaia, C. M., & Martines, J. L. Metagenomic analysis of an urban resistome before and after wastewater treatment. *Sci. Rep.* 10, 8174, doi:10.1038/s41598-020-65031-y **(2020)**.

Neuwirth, E. RColorBrewer: ColorBrewer palettes. R package version 1.1-2. https://CRAN.R-project.org/package=RColorBrewer **(2014)**.

Oh, M., Pruden, A., Chen, C., Heath, L. S., Xia, K., & Zhang, L. MetaCompare: a computational pipeline for prioritizing environmental resistome risk. *FEMS Microbiol. Ecol.* 94, fiy079, doi:10.1093/femsec/fiy079 **(2018)**.

Oksanen, J. et al. vegan: community ecology package. R package version 2.5-6. https://CRAN.R-project.org/package=vegan **(2019)**.

Pei, R. T., Kim, S. C., Carlson, K. H., & Pruden, A. Effect of River Landscape on the sediment concentrations of antibiotics and corresponding antibiotic resistance genes (ARG). *Water Res*. 40, 2427−2435, **(2006)**.

Peng, Y., Leung, H. C., Yiu, S. M., & Chin, F. Y. IDBA-UD: a de novo assembler for single-cell and metagenomic sequencing data with highly uneven depth. *Bioinformatics* 28, 1420–1428, doi:10.1093/bioinformatics/bts174 **(2012)**.

R Core Team. R: a language and environment for statistical computing. R Foundation for Statistical Computing, Vienna, Austria. URL https://www.R-project.org/ **(2018)**.

Riquelme, M.V., Garnera, E.D., Guptaa, S., Metch, J., Zhu, N.,, Blair, M.F., Arango-Argotya, G., Maile-Moskowitza, A., Flach, C.F., Aga, D.S., Nambi, I., Larsson, D.G.J., Bürgmann, H., Zhang, T., Pruden, A., Vikesland, P.J. **(in preparation)**.

Rizzo, L., Manaia, C., Merlin, C., Schwartz, T., Dagot, C., Ploy, M. C., Michael, I., & Fatta-Kassinos, D. Urban wastewater treatment plants as hotspots for antibiotic resistant bacteria and genes spread into the environment: a review. *Sci Total Environ.* 447, 345−360, doi:10.1016/j.scitotenv.2013.01.032 **(2013)**.

Singh, R. R., Angeles, L. F., Butryn, D. M., Metch, J. W., Garner, E., Vikesland, P. J., & Aga, D. S. Towards a harmonized method for the global reconnaissance of multi-class antimicrobials and other pharmaceuticals in wastewater and receiving surface waters. *Environ Int* 124, 361-369, doi:10.1016/j.envint.2019.01.025 **(2019)**.

Suzuki, M. T., Taylor, L. T., & DeLong, E. F. Quantitative analysis of small-subunit rRNA genes in mixed microbial populations via 5′- nuclease assays. *Appl Environ Microbiol* 66, 4605−4614, doi:10.1128/AEM.66.11.4605-4614.2000 **(2000)**.

Truong, D. T. et al. MetaPhlAn2 for enhanced metagenomic taxonomic profiling. *Nat. Methods* 12, 902–903, doi:10.1038/nmeth.3589 **(2015)**.

Virginia Department of Health. 2017 Virginia state and regional cumulative antibiogram. https://www.vdh.virginia.gov/content/uploads/sites/13/2018/11/2017-Virginia-State-and-Regional-Cumulative-Antibiogram.pdf **(2017)**.

Wickham, H. ggplot2: elegant graphics for data analysis. Springer-Verlag New York **(2016)**.

Wright, G. D. The antibiotic resistome: the nexus of chemical and genetic diversity. *Nature Rev. Microbiol.* 5, 175-186, doi:10.1038/nrmicro1614 **(2007)**.

Yang, Y., Li, B., Zou, S., Fang, H. H. P., & Zhang, T. Fate of antibiotic resistance genes in sewage treatment plant revealed by metagenomic approach. *Water Res*. 62, 97–106, doi:10.1016/j.watres.2014.05.019 **(2014)**.

Yin, X., Deng, Y., Ma, L., Wang, Y., Chan, L. Y. L., & Zhang, T. Exploration of the antibiotic resistome in a wastewater treatment plant by a nine-year longitudinal metagenomic study. *Environ. Int.* 133, 105270, doi:10.1016/j.envint.2019.105270 **(2019)**.

Yuan, Q. B., Guo, M. T., Wei, W. J, & Yang, J. Reductions of bacterial antibiotic resistance through five biological treatment processes treated municipal wastewater. *Environ. Sci. Pollut. Res.* 23, 19495–19503, doi:10.1007/s11356-016-7048-8 **(2016)**.

Zhang, T., Zhang, X. X., & Ye, L. Plasmid metagenome reveals high levels of antibiotic resistance genes and mobile genetic elements in activated sludge. *PLoS One* 6, e26041, doi:10.1371/journal.pone.0026041 **(2011)**.

Zhang, Y. L., Marrs, C. F., Simon, C., & Xi, C. W. Wastewater treatment contributes to selective increase of antibiotic resistance among Acinetobacter spp. *Sci. Total Environ.* 407, 3702-3706, doi:10.1016/j.scitotenv.2009.02.013 **(2009)**.

CHAPTER 3: Assessment of disinfection approaches for inactivation of antibiotic resistant *Enterococcus faecium* and *Acinetobacter baumannii* in potable reuse water

Haniyyah J. Majeed, E. Eldridge Hager Soto, Ishi Keenum, Jeanette Calarco, Marc A. Edwards, Emily D. Garner, V. Jody Harwood, and Amy Pruden

Abstract

The presence of antibiotic-resistant pathogens (ARPs) in wastewater treatment plant effluent can pose particular concern if the water is intended for reuse, as they can escape the multiple barriers of treatment including disinfection. *E. faecium* was selected to represent gram-positive cocci bacteria present in human and animal gastrointestinal tracts, and *A. baumannii* represents a gram-negative coccobacillus bacterium capable of persisting in environmental areas such as soil and surface water. The emergence of vancomycin-resistant *Enterococcus* (VRE) has caused over 5,400 deaths out of 54,400 documented infections annually in the US, while carbapenem-resistant *A. baumannii* has resulted in 700 deaths in 8,500 hospital-acquired infections. This study examined the effect of commonly applied disinfection processes (chlorination, chloramination, and ultraviolet irradiation) on the inactivation of antibiotic resistant pathogens and corresponding antibiotic susceptible pathogens in recycled water and potable water. Resistant and susceptible strains of *E. faecium* and *A. baumannii* were disinfected, and further evaluated for regrowth following disinfection by simulating conditions in distribution systems. *A. baumannii* strains were able to recover and grow especially well following UV disinfection (3-5 logs growth following 4-5 log inactivation). Meanwhile, *E. faecium* experienced a 5-6 log inactivation. *A. baumannii* strains did not regrow in the presence of a chlorine or chloramine residual, while *E. faecium* strains did not regrow following any disinfection process. There were no significant differences in results based on water type (i.e., recycled vs. potable). The findings of this study emphasize a need to move beyond the framework of assessing treatment efficacy based on the attenuation of fecal pathogens.

Introduction

Antibiotic-resistant pathogens (ARPs) can sometimes escape the multiple barriers of wastewater treatment and be detected in the effluent (Carey et al., 2016; Kulkarni et al., 2018). Presence of ARPs in wastewater treatment plant effluent can pose particular concern if the water

is intended for reuse. If the reuse water is not treated effectively to remove the ARPs, then there is potential that human populations could be exposed (Rizzo et al., 2013). In particular, disinfection is a key barrier for minimizing the presence of pathogens in wastewater effluents before they are discharged and also before it is reused, for both potable and non-potable purposes. Common disinfection strategies applied as a treatment for water reuse include: ultraviolet (UV) irradiation, chlorination, and chloramination (US EPA, 2012). However, these strategies were developed decades before the modern emphasis on the antibiotic-resistance crisis (Brodtmann & Russo, 1979; Lazarova et al., 1999). Questions have been raised with respect to which disinfection techniques are most effective for ARPs, especially in a water reuse matrix, where disinfection approaches may not be well optimized.

Water reuse is an important way to enhance water sustainability by alleviating pressure on conventional water resources and recharging them where possible. However, disinfection in water reuse scenarios poses unique challenges relative to conventional drinking water disinfection, for which disinfection technologies have generally been optimized. In particular, the greater concentration of nutrients in recycled water could interfere with disinfection, by creating disinfectant demand and resulting in disinfection by-products. Further, elevated nutrients in water reuse scenarios could increase the potential for microbial re-growth in the distribution system, relative to drinking water (Garner et al., 2016). Re-growth refers to the recovery of bacteria following disinfection and subsequent growth and increase in numbers in the distribution system. Elevated water age and extended periods of stagnation could further enhance potential for bacteria and biofilms to proliferate in water reuse distribution systems (Garner et al., 2016). Thus, there is a need to assessing the efficacy of various disinfectants on ARPs and their ability to re-grow in a recycled water matrix.

There are additional special concerns in seeking to extend disinfection practices towards addressing ARPs that could be present in wastewater effluents (Chen et al., 2015). In particular, some studies have suggested that antibiotic resistant bacteria (ARB) may be more resistant to disinfection than antibiotic-susceptible bacteria (Alexander et al., 2016) and that traditional disinfection methods of wastewater can potentially remove sensitive and resistant pathogens at different rates (Zhang et al., 2017). The general hypothesis is that some antibiotic resistance genes (ARGs) may infer cross-resistance to disinfectants. For example, multi-drug efflux pumps may also serve to help prevent entry of disinfectants entering the cell (Hou et al., 2019). If ARB also

carry greater resistance to disinfectants, this could call for tailoring the type of disinfectant added and the dose (i.e., concentration × time [C×T]). This may especially be warranted as types and numbers of ARB emitted in sewage continue to increase as a function of widespread antibiotic use in the general population. Disinfection methods that affect antibiotic-susceptible bacteria at higher rates than ARB could result in the unintentional selection of antibiotic resistance in the microbial wastewater community. An additional challenge in terms of identifying effective disinfection practices for ARPs is that resistant bacteria possess the capability to share ARGs with each other, via horizontal gene transfer. Thus, even if ARB are killed or inactivated, the potential remains that the ARGs could remain functional and be transferred to new bacterial hosts. Transfer to bacterial pathogens, rendering them ARPs, is especially of concern. Thus, disinfection strategies that destroy ARGs (McKinney & Pruden, 2012; Yoon et al., 2017; Yoon et al., 2018), or at least avoid stimulating horizontal gene transfer, are desirable.

The two ARPs selected for this study are *Enterococcus faecium* and *Acinetobacter baumannii*. *E. faecium* was selected to represent gram-positive cocci bacteria present in human and animal gastrointestinal tracts, and *A. baumannii* represents a gram-negative coccobacillus bacterium capable of persisting in environmental areas such as soil and surface water. Both of these microorganisms additionally serve as examples of current significant sources for nosocomial infections with high potential for acquiring ARGs from their environment (Fisher & Phillips, 2009; Eliopoulus, Maragakis, & Perl, 2008). The emergence of vancomycin-resistant *Enterococcus* (VRE) has caused over 5,400 deaths out of 54,400 documented infections in the United States of America in 2017 (US CDC, 2019). *Enterococcus* spp. constitutes a significant part of the microbiota of humans' GI tract; however, most hospital-acquired infections of VRE result from spread from the hands of hospital personnel rather than endogenous bacteria (Weinstein & Hayden, 2000). VRE mainly manifests as bacteremia and endocarditis, both conditions commonly acquired due to *Enterococcus* infection of the urinary tract (Agudelo Higuita & Huycke, 2014). Likewise, carbapenem-resistant *A. baumannii* poses a serious public health risk resulting in 700 deaths in 8,500 hospital-acquired infections in the United States in 2017 (US CDC, 2019). Unlike *Enterococcus*, *A. baumannii* both represents a member of humans' microbiota in addition to holding environmental reservoirs in soil (Dijkshoorn, Nemec & Seifert, 2007; Berlau et al., 1999). Infection by *A. baumannii* occurs frequently in hospital patients, especially those in critical condition and those under intensive care for extended periods of time (McConnell, Actis, &

Pachón, 2013). *A. baumannii*'s propensity for obtaining multidrug resistance and its ability to remain viable on dry surfaces for long periods of time contribute to the increasing risk this pathogen imposes in hospital settings (Jawad et al., 1998; Perez et al., 2007).

The objective of this study was to compare three disinfectants: chlorine, chloramine, and UV irradiation in terms of their efficacy for inactivating *E. faecium* and *A. baumannii* in water intended for reuse and distribution. These organisms were selected to provide contrast in terms of representing a gram-positive fecal pathogen (*E. faecium*) and a gram-negative environmental pathogen (*A. baumannii*) that can both be found in wastewater. To assess variation among strains and whether antibiotic resistance or susceptibility plays a role in inactivation kinetics, we characterized the inactivation rates of representative susceptible and resistant strains of each microorganism as a function of C×T for each disinfectant. Further, we examined the potential for these pathogens to survive and regrow following disinfection and simulated distribution. Experiments were conducted in both recycled water and conventional drinking water matrices to assess whether recycled water potentially interferes with disinfection or stimulates regrowth. While this study was not designed to definitively determine if antibiotic resistance enhances resistance to disinfectants, it does provide insight into the general efficacy of disinfectants and ranges of C×Ts that may be required to ensure that key ARPs are inactivated and inhibited from re-growing in water reuse distribution systems.

Materials and methods

Preparation of water samples

Final effluent water from both the Virginia and Florida water reclamation facilities were collected during the time of sampling and transported to Virginia Tech. The Florida reclaimed water treatment facility produces 31.5 MGD of water intended for non-potable reuse treated by primary settling, activated sludge, secondary clarification, denitrifying filtration, and UV disinfection. The Virginia reclaimed water treatment facility produces 1 MGD of water intended for indirect potable reuse by the following processes, including advanced treatment: primary settling, activated sludge, and secondary clarification, ozonation, biologically active filtration, granular activated carbon, and UV disinfection.

Table 3-1. Physiochemical parameters of test waters.

	Florida Reuse Water	Florida Potable Water	Virginia Reuse Water	Virginia Potable Water
pH	7.74	8.01	7.75	7.74
Dissolved Oxygen	8.69	8.00	8.63	8.80
Ammonia (mg/L)	0.06	0.56	0.22	0.54
Temperature (°C)	26.1	24.8	26.7	26.7
UV_{254} absorbance	0.093	0.06	0.051	0.006

The following physiochemical parameters were measured in each test water: pH, dissolved oxygen (DO), ammonia, temperature, and UV_{254} absorbance (Table 3-1). pH was measured using an Oakton 110 Series pH meter (Cole-Parmer, Count Vernon Hills, IL). DO was measured using an Orion Star A223 meter (Thermo Scientific, Waltham, MA). Ammonia was measured using Standard Method 5310-NH3 and UV_{254} absorbance using Standard Method 10054 on a DR5000 spectrophotometer (HACH, Loveland, CO). Concurrently, potable water from a tap at each respective facility was collected. Upon arrival, water was stored at 4 °C. Prior to use for the experiment, each water was aliquoted in sterile, 500-mL Pyrex bottles and pasteurized by maintaining the waters at 70 °C for at least 30 minutes in a water bath. Waters were allowed to reach room temperature before inoculation.

Preparation of bacterial suspensions and culture conditions

The clinical strain *A. baumannii* American Type Culture Collection (ATCC) ATCC BAA-1789 was isolated from tracheal aspirate of a human patient in 2008. While this strain has resistance to multiple antimicrobials, it is considered to be the antibiotic "susceptible" strain due to its susceptibility specifically to imipenem at the target concentration of 3 μg/mL utilized in this study. The clinical strain *A. baumannii* ATCC BAA-2802 was isolated from a human blood sample in 2014 and is considered to be "highly" multidrug-resistant. The resistant and susceptible *A. baumannii* strains were cultured in tryptic soy broth (TSB) with or without 3 μg/mL imipenem, respectively. The plasmid-bearing *E. faecium* strain, E0292 (Young, Rohr, & Harwood, 2019), isolated from human urine features vancomycin resistance gene, *van*A. The antibiotic sensitive strain utilizied in this study was *E. faecium* 64/3 (Young, Rohr, & Harwood, 2019). The resistant

and susceptible *E. faecium* strains were cultured in brain heart infusion (BHI) broth with or without 4 μg/mL vancomycin, respectively. Strains were grown in cultures overnight at 37 °C for *A. baumannii* strains and 41 °C for *E. faecium* strains. Cells were harvested by centrifugation (5000 g for 30 min, followed by 5000 g for 5 min twice), washed twice in 10 mM sterile phosphate buffer solution, and resuspended.

Sensitive and resistant strains of both *E. faecium* and *A. baumannii* were inoculated at a target concentration of 10^6 CFU/mL each into all test waters and immediately cultured for initial colony counts. Disinfected waters were enumerated on media without antibiotics as a measure of total sensitive and resistant strains and on media with antibiotics as a measure of total resistant strains. The selective media used for culturing *A. baumannii* and *E. faecium* were CHROMagar Acinetobacter (with or without 3 μg/mL imipenem) and mEI (with or without 4 μg/mL vancomycin), respectively. For enumeration of colony counts, waters were filter concentrated using 47 mm 0.45 μm pour size mixed cellulose ester membrane filters (VWR, Radnor, PA).

UV Trials

Following inoculation and initial culturing, approximately 80 mL of each water was transferred to a glass Petri dish on a stir plate and irradiated at a target dose of 100 mJ/cm^2 using a collimated beam apparatus until the total volume was irradiated. Following disinfection, waters were incubated in the dark at room temperature in a sealed glass jar with adequate headspace at 100 rpm to stimulate distribution. Three samples were taken for culturing over the 5-day period: prior to UV irradiation, following UV irradiation, and after 5 days.

Chlorine and Chloramine Trials

The chlorine and chloramine disinfection experiments were conducted together, with chlorine serving as the primary disinfectant for both, followed by adjustment to represent chlorine secondary residual versus chloramine secondary residual for the distribution simulation portion of the experiments. Free and total chlorine were measured using Standard Method 4500-Cl2, using a DR5000 spectrophotometer (HACH, Loveland, CO). A C×T value of 450 mg-min/L free chlorine was targeted prior to a 5-day regrowth phase growth in the dark at room temperature in a sealed glass jar with adequate headspace at 100 rpm for both chlorine and chloramine trials. The target dose of 3 mg/L free chlorine was selected to reach the C×T value within 150 minutes. However,

with free chlorine decay in the test waters over time, free chlorine levels had to be continuously monitored in real-time to create a chlorine curves simplified to zero-order decay for the purpose of rapidly updating the ongoing C×T value by calculating the area under the curve. When free chlorine levels fell below 2 mg/L, additional free chlorine was added. Once the target C×T was achieved, the test waters were split into approximately equal volumes for the 5-day regrowth phase in the dark at room temperature at 100 rpm. The final chlorine residual was held in one set of the test waters, while ammonia was dosed in the other set to create a chloramine residual, measured as total chlorine. In some instances, adequate enumeration was not available for some strains, thus the average and standard deviation of all the previous trials, including preliminary trials, was used as the initial starting value.

Statistical analysis and data visualization

Where applicable, Wilcoxon rank-sum tests were utilized using the wilcox.test() in R version 3.5.1 (R Core Team, 2018) with the built-in stats package to determine statistical differences between strains. A significance level of $\alpha = 0.05$ was used for all statistical analyses. All graphics were generated using ggplot2 (Wickham, 2016) and RColorBrewer (Neuwirth, 2014) in R.

Results

UV Disinfection

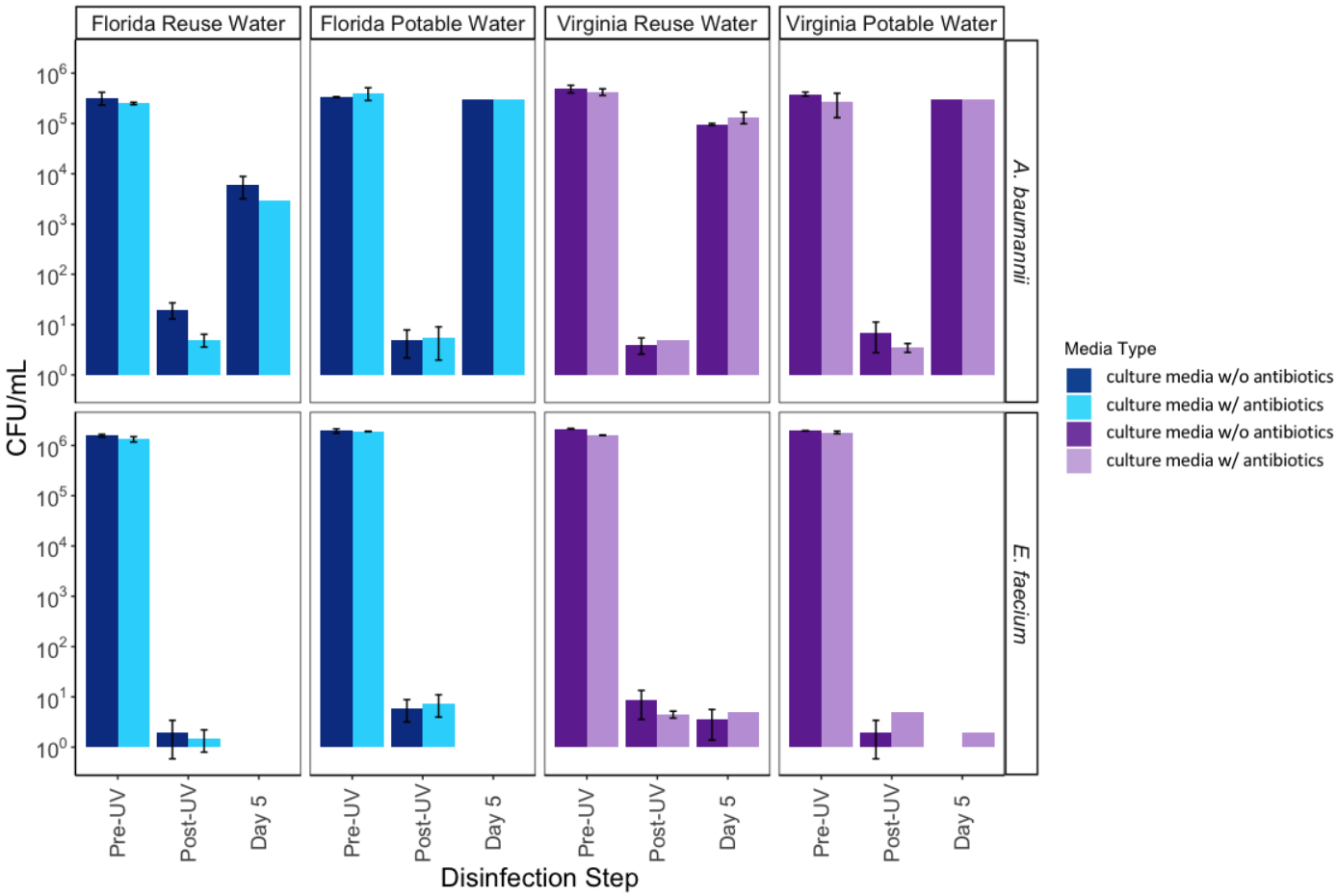

Figure 3-1. Culture results from disinfectant trial of UV irradiation at 100 mJ/cm^2.

Blue bars represent test waters from Florida; purple bars represent test waters from Virginia; lighter bars represent culture data from agar supplemented with antibiotics; darker bars represent culture data from agar not supplemented with antibiotics. Day 5 indicates numbers enumerated after incubating in the water an additional 5 days to simulate re-growth conditions during distribution. Limits of detection: pre-UV (3×10^4 CFU/mL), post-UV (3 CFU/mL), and Day 5 (3×10^5 CFU/mL).

Following UV disinfection at 100 mJ/cm^2, 4-5 log inactivation of *A. baumannii* was achieved and 5-6 log inactivation of *E. faecium* was achieved (Figure 3-1). The resistant and sensitive strains appeared to generally be affected equally, with slightly higher CFUs of *A. baumannii* enumerated on media without antibiotics for the Florida reuse water, although not significantly higher ($p = 0.333$). The most striking result in terms of UV disinfection was that, for all water conditions, *A. baumannii* demonstrated strong potential for re-growth. For three of the

four waters tested, *A. baumannii* re-grew to levels equivalent to the initial levels, while in the Florida reuse water A. baumannii re-grew by 3 logs (Figure 3-1, $p = 0.029$). *E. faecium*, on the other hand, did not re-grow under any of the conditions, and after five days of incubation it was below quantification in three of the four waters, although it persisted at the post-UV level in the Virginia reuse water (Figure 3-1).

Chlorine and Chloramine Disinfection

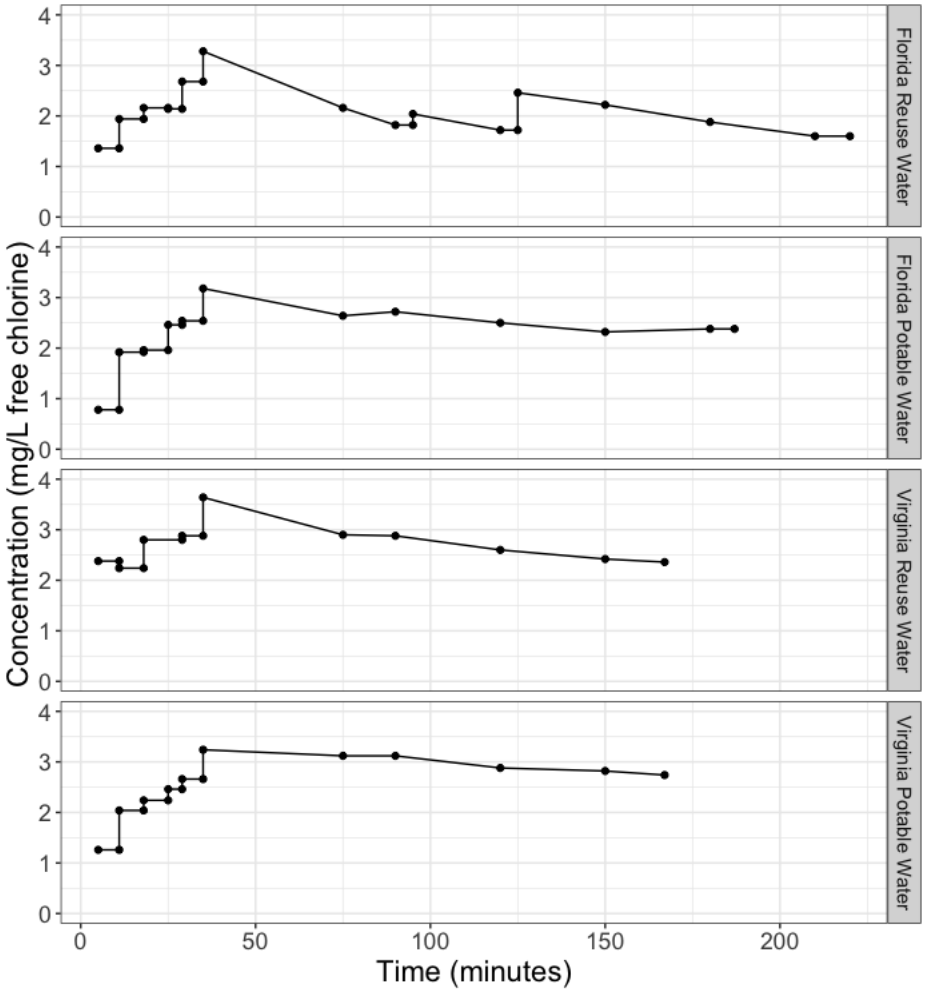

Figure 3-2. Chlorine primary disinfection curves (concentration measured as mg/L free chlorine) as a function of time to reach target C×T of ~450 mg-min/L in all four waters.

The chlorine and chloramine disinfection experiments were conducted together, with chlorine serving as the primary disinfectant for both, followed by adjustment to represent chlorine secondary residual versus chloramine secondary residual for the distribution simulation portion of

the experiments. Chlorine disinfection curves were developed for the chlorine and chloramine disinfection experiments for each of the four waters (Figure 3-2).

Table 3-2. Parameters of test waters undergoing chlorine and chloramine disinfection.

	Florida Reuse Water	Florida Potable Water	Virginia Reuse Water	Virginia Potable Water
Theoretical chlorine dose (mg/L)	10.5	7.5	10.0	9.0
Final CT value (mg-min/L)	453	450	451	460
Final free chlorine (mg/L)	1.6	2.36	2.38	2.74
Total free chlorine demand (mg/L)	8.9	5.14	7.62	6.26
Chlorinated samples				
Final free chlorine (mg/L)	2.08	2.36	2.38	2.74
After 5 days: free chlorine (mg/L)	0.77	0.34	0.78	0.70
Chloraminated samples				
Final free chlorine (mg/L)	2.08	2.36	2.38	2.74
Total chlorine after ammonia dosing (mg/L)	2.72	2.58	2.6	2.56
Free chlorine after ammonia dosing (mg/L)	0.38	0.2	0.3	0.61
After 5 days: total chlorine (mg/L)	2.89	2.4	2.89	2.79

As expected, each water was distinct in chemistry exerted distinct disinfection demands, with the reuse waters incurring a slightly higher demand (Table 3-2). The demand curves were used to ensure that a consistent C×T of ~450 mg-min/L was applied across the four waters before commencing the distribution simulation. The initial targeted dose prior to distribution was ~2 mg/L for both disinfectants. It was found that chlorine was more reactive and decayed to a greater extent across all waters, while chloramine was more stable in all waters after 5 days of distribution stimulation (Table 3-2).

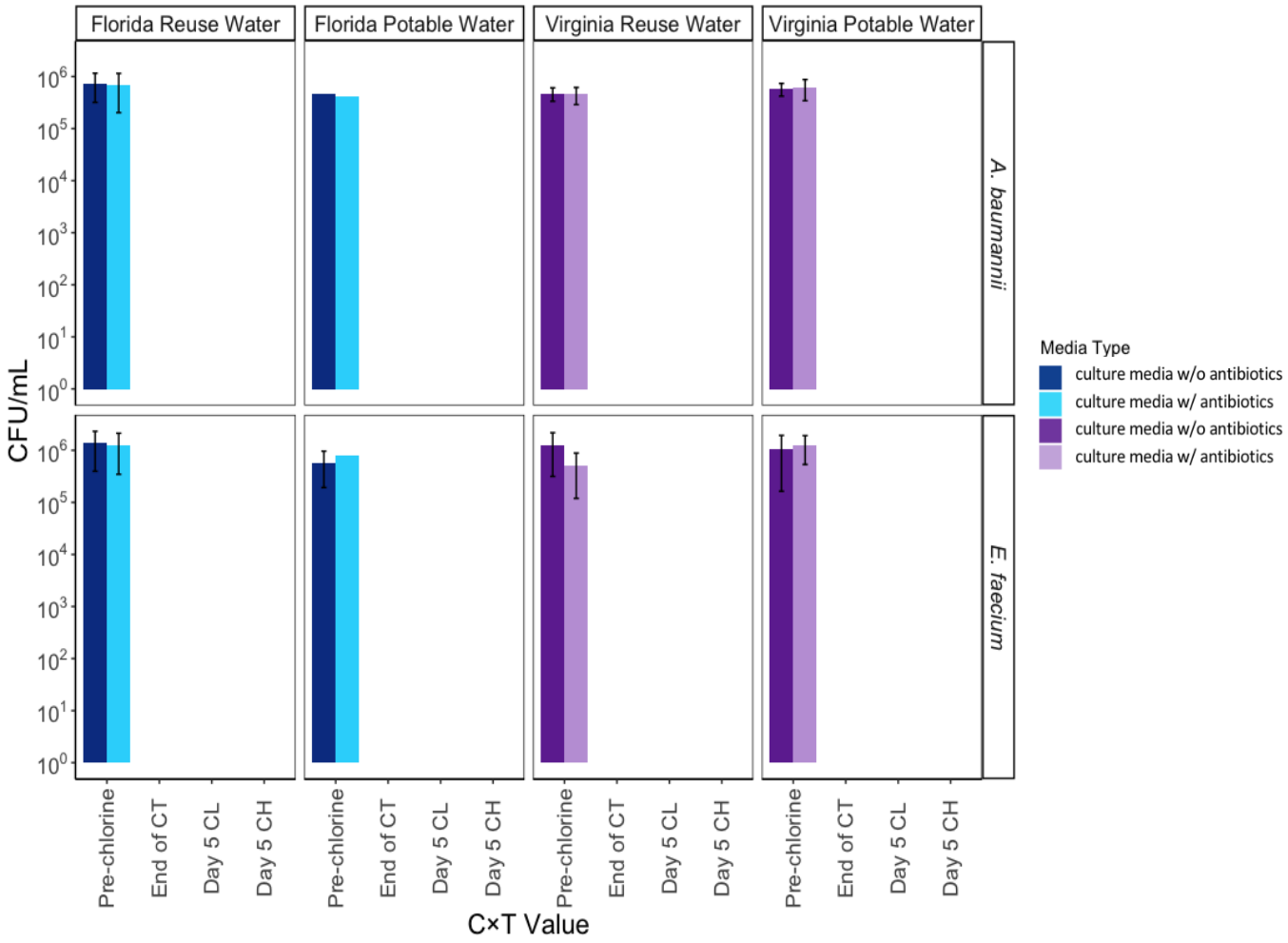

Figure 3-3. Culture results from chlorine primary disinfection followed by the use of chlorine or chloramine as a secondary residual.

Primary disinfection utilized free chlorine at CT of approximately 450 mg-min/L followed by simulated distribution with addition of either free chlorine or chloramine secondary residual at a target concentration of 2 mg/L and testing after 5 days. Blue bars represent test waters from Florida; purple bars represent test waters from Virginia; lighter bars represent culture data from agar supplemented with antibiotics; darker bars represent culture data from agar not supplemented with antibiotics. Limits of detection: pre-chlorine (3×10^4 CFU/mL), End of C×T (3×10^{-1} CFU/mL), and Day 5 (6×10^{-2} CFU/mL). **CL** = chlorine; **CH** = chloramine.

In general, it was found that chlorine primary disinfection resulted in reduction of all four pathogens strains below detection for all four waters (Figure 3-3). None of the strains recovered in any of the four waters under the simulated distribution conditions, even though free chlorine secondary disinfection had reduced by the end of the experiment to < 0.8 (but >0.3) mg/L by the end of the incubation experiment. On the other hand, chloramine secondary disinfection resulted

in a total chlorine residual >2.4 mg/L and free chlorine concentration >0.2 mg/L (Table 3-2), thus sustaining an effective concentration to inhibit regrowth.

Comparison between A. baumannii and E. faecium

After five days of simulated distribution, it was quite notable that *A. baumannii* persisted at equivalent levels to those observed immediately after chlorine primary disinfection (i.e., below detection) or regrew to levels equal to or greater than the concentration at initial inoculation following UV disinfection. *E. faecium*, on the other hand, was already reduced to very low levels and tended to reduce even further or be non-detectable following 5 days of simulated distribution conditions.

Discussion

This study provided a helpful overview of the expected range of efficacy of three disinfectants applied for control of ARPs that could be present in waters intended for reuse. In general, it was found that *E. faecium* was readily inactivated by all three disinfectants and did not indicate signs of re-growth during 5 days of simulated distribution conditions. However, *A. baumannii* was less readily activated than *E. faecium* by UV and also increased during this period following UV treatment to initial levels. The different behavior of these strains is consistent with the understanding that *A. baumannii* is an environmentally-adapted organism and thus more amenable to survival and regrowth in the distribution system than the fecally-derived Enterococcus. *E. faecium* was selected to represent gram-positive cocci bacteria present in human and animal gastrointestinal tracts (Fisher & Phillips, 2009), and *A. baumannii* represents a gram-negative coccobacillus bacterium capable of persisting in environmental areas such as soil and surface water (Eliopoulus, Maragakis, & Perl, 2008). The findings of this study have important implications for control of other opportunistic pathogens in recycled water distribution systems, such nontuberculous mycobacteria, *Pseudomonas aeruginosa*, and *Legionella* spp. A concerted effort to tailor recycled water disinfection and distribution practices to address environmental opportunistic pathogens capable of regrowth in distribution systems would be of value.

Ideally, under multi-barrier conditions of wastewater treatment followed by water reuse treatments, there would be few opportunities for ARPs to penetrate and proliferate. However, it is important to ensure that disinfection strategies are tailored to address ARPs in the case that they do, while also avoiding selection pressures that could lead to enhanced survival of environmental

opportunistic ARPs through treatment and distribution. Overall, this study demonstrated that free chlorine primary disinfection, followed by chlorine or chloramine secondary residual was by far the most effective for eliminating both ARPs below disinfection and preventing their re-growth, as observed in previous studies (Sullivan et al., 2017). This is an interesting finding, given recent reports that chlorine-based disinfectants can select for antibiotic resistance (Templeton et al., 2009; Karumathil et al., 2014; Liu et al., 2018). However, important to emphasize in this study is that the conditions employed were meant to represent ideal target disinfection and operating conditions, with typical primary and secondary disinfection doses. In future studies, it would be of interest to explore what might happen if sub-optimal disinfection conditions are employed. In particular, it would be of interest to examine if ARPs recover and regrow under the worst-case-scenario of absence of chlorine-based disinfectant residual. Bédard et al. (2014) observed that viability of *Pseudomonas aeruginosa* was regained almost immediately following disinfection, while culturability was regained once the chlorine residual was depleted. Similarly, *A. baumannii* persisted and re-grew in this study in the UV condition, in which disinfectant residuals were absent.

Because the two representative strains employed in this study differed by more than just their antibiotic resistance characteristics, it is important not to over-interpret the results that any differences in strain behavior were explicitly due to their resistance properties. Indeed, different strains of the same species of bacteria often intrinsically differ in their disinfection kinetics independent of their antibiotic resistance status (Silverman & Nelson, 2016). Often it is found that environmental strains are more difficult to disinfect than clinical strains. Future studies would benefit from examining a wider variety of strains in order to gain stronger evidence for the role of antibiotic resistance as a mediator that increases disinfectant resistance. Another approach would be to employ isogenic strains with knock-out mutations, to demonstrate for certain that a specific ARG is involved in disinfectant resistance.

Acknowledgements

We would like to thank the reuse facilities for allowing us to collect water for our experiments. This study was supported by Centers for Disease Control and Prevention (CDC) contract 75D30118C02904. The National Science Foundation NNCI award 1542100 and the Center for Science and Engineering of the Exposome at the Virginia Tech Institute for Critical Technology and Applied Science (ICTAS) provided internal support for this work.

References

Alexander, J., Knopp, G., Dötsch, A., Wieland, A. & Schwartz, T. Ozone treatment of conditioned wastewater selects antibiotic resistance genes, opportunistic bacteria, and induce strong population shifts. *Sci. Total Environ.* 559, 103-112 doi:10.1016/j.scitotenv.2016.03.154 **(2016)**.

Bédard, E., Charron, D. Lalancette, C., Déziel, E., & Prévost, M. Recovery of *Pseudomonas aeruginosa* culturability following copper- and chlorine-induced stress. *FEMS Microbiol. Lett.* 356, 226–234, doi:10.1111/1574-6968.12494 **(2014)**.

Berlau, J., Aucken, H. M., Houang, E., & Pitt, T. L. Isolation of *Acinetobacter* spp. including *A. baumannii* from vegetables: implications for hospital-acquired infections. *J. Hosp. Infect.* 42, 201-204 doi:10.1053/jhin.1999.0602 **(1999)**.

Brodtmann Jr., N. V., & Russo, P. J. The use of chloramine for reduction of trihalomethanes and disinfection of drinking water. *J. Am. Water. Works. Assoc.* 71, 40-42 **(1979)**.

Carey,S. A., Rosenburg Goldstein, R. E., Gibbs, S. G., Claye, E., He, X., & Sapkota, A. Occurrence of vancomycin-resistant and -susceptible *Enterococcus* spp. in reclaimed water used for spray irrigation. *Environ. Res.* 147, 350-355, doi:10.1016/j.envres.2016.02.030 **(2016)**.

Chen, J., et al. Removal of antibiotics and antibiotic resistance genes in rural wastewater by an integrated constructed wetland. *Environ. Sci. Pollut. Res.* 22, 1794–1803, doi:10.1007/s11356-014-2800-4 **(2015)**.

Dijkshoorn, L., Nemec, A., & Seifert, H. An increasing threat in hospitals: multidrug-resistant *Acinetobacter baumannii*. *Nat. Rev. Microbiol* 5, 939-951 doi:10.1038/nrmicro1789 **(2007)**.

Eliopoulos, G. M., Maragakis, L. L., Perl, T. M. *Acinetobacter baumannii*: epidemiology, antimicrobial resistance, and treatment options. *Clinical infectious diseases* 46, 1254-1263, doi:10.1086/529198 **(2008)**.

Fisher, K. & Phillips, C. The ecology, epidemiology and virulence of *Enterococcus*. *Microbiol.* 155, 1749-1757, doi:10.1099/mic.0.026385-0 **(2009)**.

Garner, E. et al. Impact of blending for direct potable reuse on premise plumbing microbial ecology and regrowth of opportunistic pathogens and antibiotic resistant bacteria. *Water Res.* 151, 75-86, doi:10.1016/j.watres.2018.12.003 **(2019)**.

Garner, E., Zhu, N., Strom, L., Edwards, M., & Pruden, A. A human exposome framework for guiding risk management and holistic assessment of recycled water quality. *Environ. Sci.* 2, 580-598, doi:10.1039/C6EW00031B **(2016)**.

Agudelo Higuita, N. I. & Huycke, M. M. Enterococcal disease, epidemiology, and implications for treatment. *Enterococci*: from commensals to leading causes of drug resistant infection [Internet]. Massachusetts Eye and Ear Infirmary **(2014)**.

Hou, A., et al. Chlorine injury enhances antibiotic resistance in Pseudomonas aeruginosa through over expression of drug efflux pumps. *Water Res.* 156, 366-371, doi:10.1016/j.watres.2019.03.035 **(2019)**.

Jawad, A., Seifert, H., Snelling, A. M., Heritage, J., & Hawkey, P. M. Survival of *Acinetobacter baumannii* on dry surfaces: comparison of outbreak and sporadic isolates. *J Clin. Microbiol.* 36, 1938-1941, doi:10.1128/JCM.36.7.1938-1941.1998 **(1998)**.

Karumathil, D. P., Yin, H., Kollanoor-Johny, A., & Venkitanarayanan, K. Effect of chlorine exposure on the survival and antibiotic gene expression of multidrug resistant *Acinetobacter baumannii* in water. *Int. J. Environ. Res. Public Health* 11, 1844-1854, doi:10.3390/ijerph110201844 **(2014).**

Kulkarni, P. et al. Conventional wastewater treatment and reuse site practices modify bacterial community structure but do not eliminate some opportunistic pathogens in reclaimed water. *Sci. Total Environ.* 639, 1126-1137, doi:10.1016/j.scitotenv.2018.05.178 **(2018)**.

Lazarova, V., Savoye, P., Janex, M. L., Blatchley III, E. R. & Pommepuy, M. Advanced wastewater disinfection technologies: state of the art and perspectives. *Water Sci. Technol.* 40, 203-213, doi:10.1016/S0273-1223(99)00502-8 **(1999)**.

Liu, S.-S. et al. Chlorine disinfection increases both intracellular and extracellular antibiotic resistance genes in a full-scale wastewater treatment plant. *Water Res.* 136, 131-136, doi:10.1016/j.watres.2018.02.036 **(2018)**.

McConnell, M. J., Actis, L., & Pachón, J. *Acinetobacter baumannii*: human infections, factors contributing to pathogenesis and animal models. *FEMS Microbiol. Rev.* 37, 130-155, doi: 10.1111/j.1574-6976.2012.00344.x **(2013)**.

McKinney, C. & Pruden, A. Ultraviolet disinfection of antibiotic resistant bacteria and their antibiotic resistance genes in water and wastewater. *Environ. Sci. Technol.* 46, 13393–13400, doi:10.1021/es303652q, **(2012)**.

Neuwirth, E. RColorBrewer: ColorBrewer palettes. R package version 1.1-2. https://CRAN.R-project.org/package=RColorBrewer **(2014)**.

Federico, P., Hujer, A. M., Hujer, K. M., Decker, B. K., Rather, P. N., & Bonomo, R. A. Global challenge of multidrug-resistant *Acinetobacter baumannii*. *Antimicrob. Agents Chemo.* 51, 3471-3484, doi:10.1128/AAC.01464-06 **(2007)**.

R Core Team. R: a language and environment for statistical computing. R Foundation for Statistical Computing, Vienna, Austria. URL https://www.R-project.org/ **(2018)**.

Rizzo, L., Manaia, C., Merlin, C., Schwartz, T., Dagot, C., Ploy, M. C., Michael, I., & Fatta-Kassinos, D. Urban wastewater treatment plants as hotspots for antibiotic resistant bacteria and

genes spread into the environment: a review. *Sci Total Environ.* 447, 345−360, doi:10.1016/j.scitotenv.2013.01.032 **(2013)**.

Silverman, A. I. & Nelson, K. L. Modeling the endogenous sunlight inactivation rates of laboratory strain and wastewater *E. coli* and Enterococci using biological weighting functions. *Environ. Sci. Technol.* 50, 12292-12301, doi:10.1021/acs.est.6b03721 **(2016).**

Sullivan, B. A., Vance, C. C., Gentry, T. J., & Karthikeyan, R. Effects of chlorination and ultraviolet light on environmental tetracycline-resistant bacteria and tet(W) in water. *J. Environ. Chem. Eng.* 5, 777-784, doi:10.1016/j.jece.2016.12.052 **(2017)**.

Templeton, M. R., Oddy, F., Leung, W., & Rogers, M. Chlorine and UV disinfection of ampicillin-resistant and trimethoprim-resistant *Escherichia coli. Can. J. Civ. Eng.* 36, 889-894, doi:10.1139/L09-040 **(2009).**

United States Centers for Disease Control and Prevention. Antibiotic Resistance Threats **(2019).**

United States Environmental Protection Agency. Guidelines for Water Reuse **(2012)**.

Weinstein, R. A. & Hayden, M. K. Insights into the epidemiology and control of infection with vancomycin-resistant enterococci. *Clin. Infect. Dis.* 31, 1058-1065, doi:10.1086/318126 **(2000)**.

Wickham, H. ggplot2: elegant graphics for data analysis. Springer-Verlag New York **(2016)**.

Yoon, Y., Dodd, M. C., & Lee, Y. Elimination of transforming activity and gene degradation during UV and UV/H2O2 treatment of plasmid-encoded antibiotic resistance genes. *Environ. Sci.: Water Res. Technol.* 4, 1239, doi:10.1039/c8ew00200b **(2018).**

Yoon, Y., Chung, H. J., Wen Di, D. Y., Dodd, M. C., Hur, H. G., & Lee, Y. Inactivation efficiency of plasmid-encoded antibiotic resistance genes during water treatment with chlorine, UV, and UV/H2O2. *Water Res.* 123, 783-793, doi:10.1016/j.watres.2017.06.056 **(2017)**.

Young, S., Rohr, J. R., & Harwood, V. J. Vancomycin resistance plasmids affect persistence of *Enterococcus faecium* in water. *Water Res.* 166, 115069, doi:10.1016/j.watres.2019.115069 **(2019).**

Zhang, C. M., Xu, L. M., Wang, X. C., Zhuang, K., & Liu, Q. Q. Effects of ultraviolet disinfection on antibiotic-resistant *Escherichia coli* from wastewater: inactivation, antibiotic resistance profiles and antibiotic resistance genes. *J. Appl. Microbiol.* 123, 295-306, doi:10.1111/jam.13480 **(2017).**

Appendix A - Supplemental Material for Chapter 2

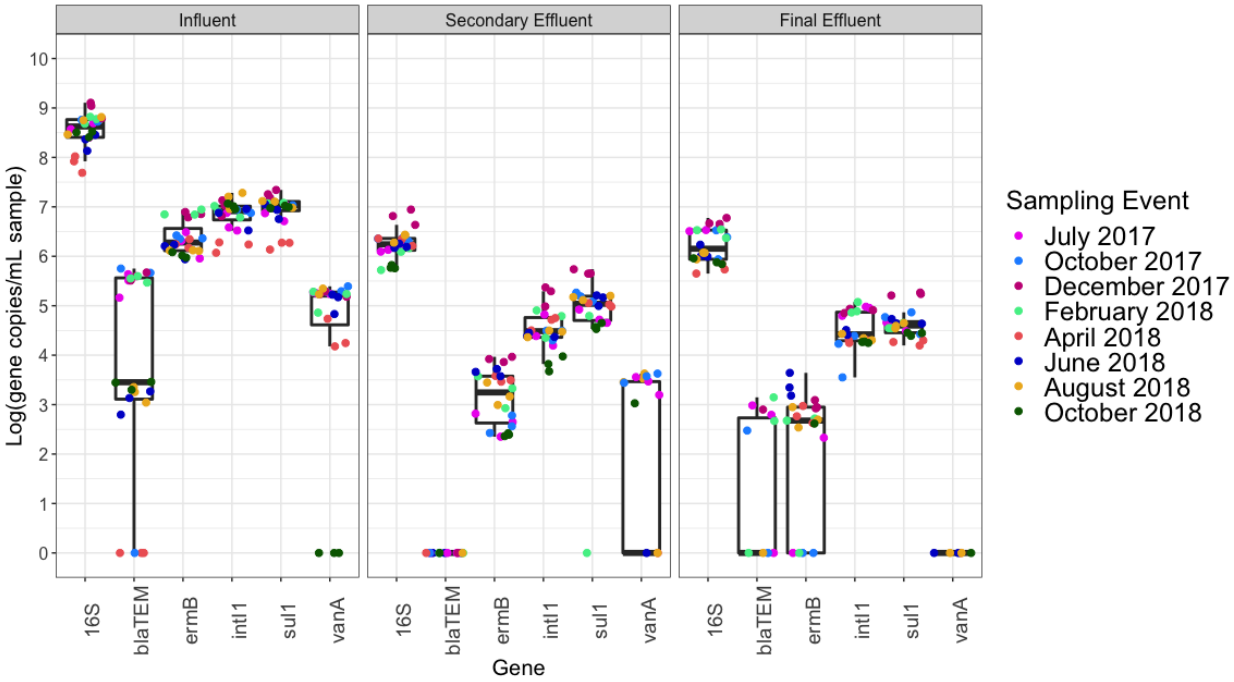

Supplementary Figure 1. Absolute abundance (as log gene copies per mL of sample) of select ARGs, a class 1 integron integrase gene, and total bacterial 16S rRNA genes in the influent, secondary effluent, and final effluent measured by qPCR.

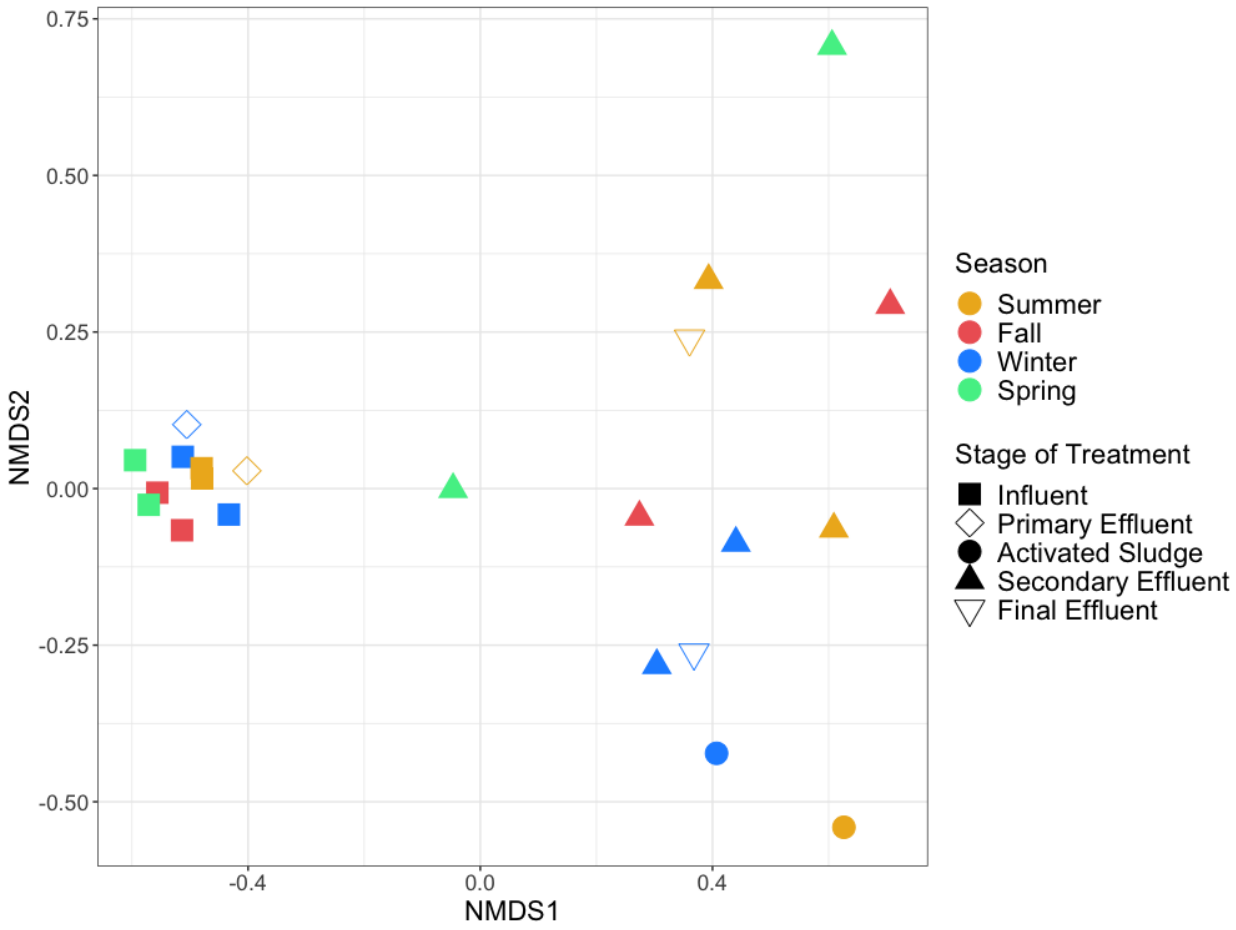

Supplementary Figure 2. NMDS analysis of ARG profiles based on relative abundance across WWTP sampling locations and seasons according to shotgun metagenomic sequencing. Influent samples did not exhibit distinct separation based on relative abundance of ARGs when grouped by season (ANOSIM; #ARGS = 859, R = 0.1458, p = 0.241), likewise secondary effluent samples were not separated by season (ANOSIM; #ARGS = 637, n = 2, R = -0.1667, p = 0.785). ARGs were annotated via CARD (Jia et al., 2017).

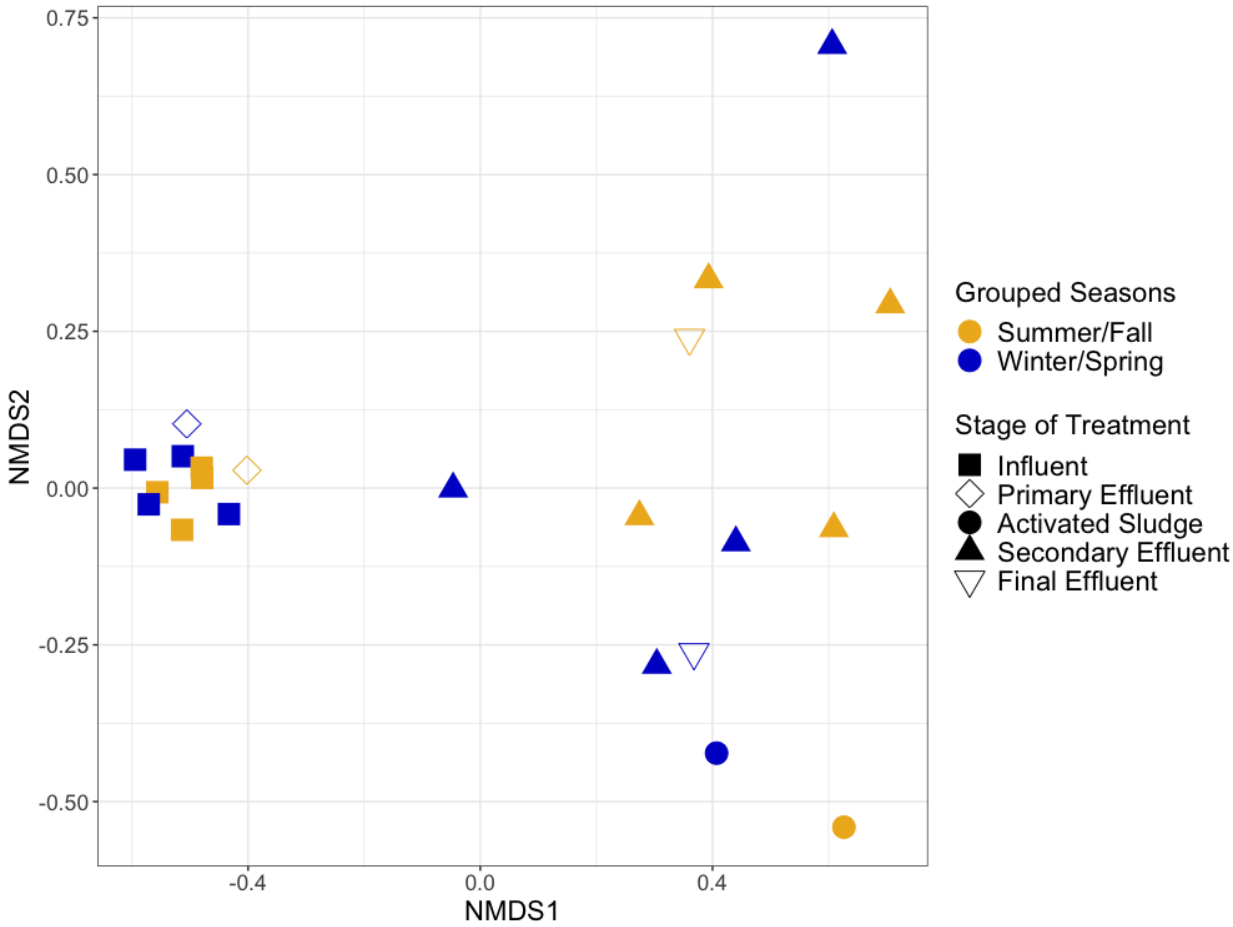

Supplementary Figure 3. NMDS analysis of ARG profiles based on relative abundance across WWTP sampling locations and grouped seasons according to shotgun metagenomic sequencing. Influent samples did not exhibit distinct separation based on relative abundance of ARGs based on grouped seasons (ANOSIM; #ARGS = 859, R = 0.2396, p = 0.064), likewise secondary effluent samples were not separated by grouped seasons (ANOSIM; #ARGS = 637, n = 4, R = -0.04167, p = 0.63). ARGs were annotated via CARD (Jia et al., 2017).

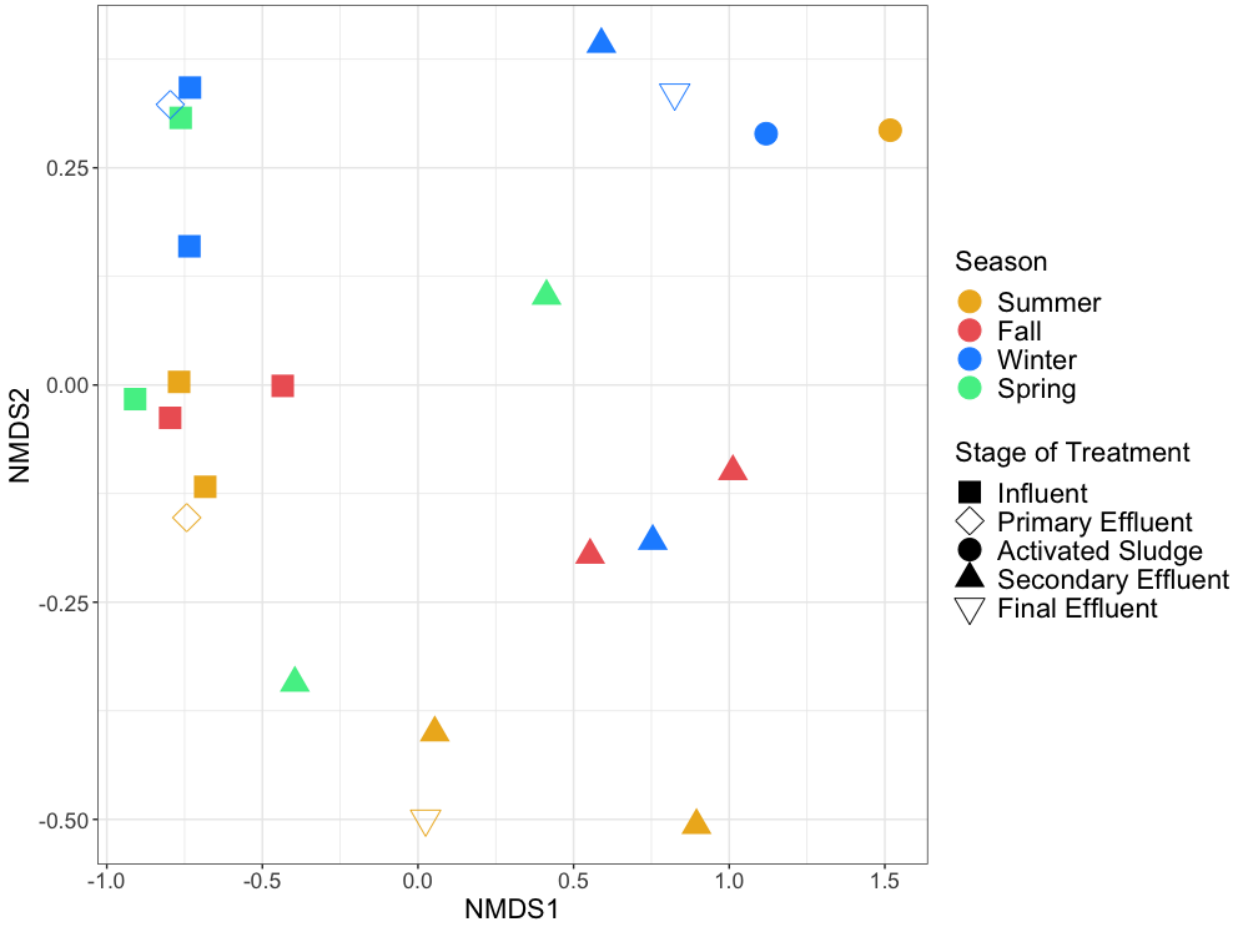

Supplementary Figure 4. NMDS analysis of taxonomic profiles at genus level across WWTP sampling locations and seasons according to shotgun metagenomic sequencing. Influent samples did not exhibit distinct separation based on genus level relative abundance by season (ANOSIM; R = 0.5208, p = 0.04), likewise secondary effluent samples were not separated by season (ANOSIM; R = -0.1458, p = 0.775). Taxonomy was annotated via MetaPhlAn2 (Truong et al., 2015).

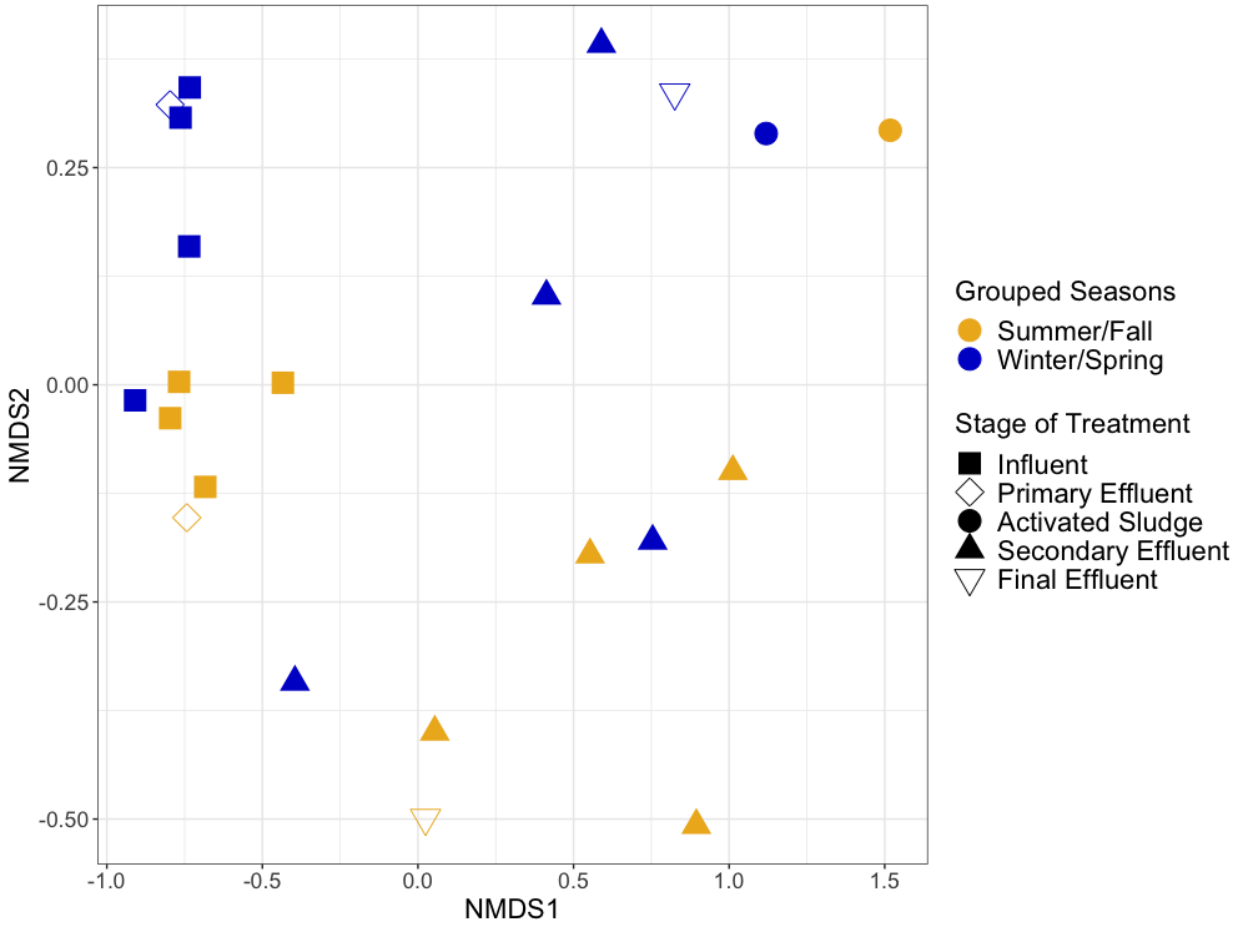

Supplementary Figure 5. NMDS analysis of taxonomic profiles at genus level across WWTP sampling locations and grouped seasons according to shotgun metagenomic sequencing. Influent samples did not exhibit distinct separation based on genus level relative abundance by grouped seasons (ANOSIM; R = 0.1354, p = 0.213), likewise secondary effluent samples were not separated by grouped seasons (ANOSIM; R = -0.1146, p = 0.789). Taxonomy was annotated via MetaPhlAn2 (Truong et al., 2015).

Supplementary Table 1. Sampling data and notes corresponding to each sampling event

Date	Ambient Temperature (°C)	Stage of Treatment	Temperature of Sample (°C)	Dissolved Oxygen (mg/L)	pH	TSS (mg/L)[a,b]	BOD (mg/L)[a,b]
2017-07-19	22[c]	Influent	20.6	3.31	6.94	215	-
		Secondary Effluent	23.1	2.06	6.27	5.9, 2.5	3.8, 3.7
2017-10-17	13	Influent	19.8	3.18	6.95	220	-
		Secondary Effluent	20.1	3.63	6.56	4.4, 8.9	
2017-12-14	3[c]	Influent	14.1	5.65	7.7	200	-
		Secondary Effluent	12.7	2.4	6	10.1, 10.7	10.8, 10
2018-02-21	19 [c]	Influent	11.8	7.05	7.65	215	-
		Primary Effluent	11.8	5.08	6.96	-	-
		Activated Sludge	12.7	0.43	6.27	-	-
		Secondary Effluent	12.7	3.6	6.32	7.1, 4.7	6.1, 4.7
		Final Effluent	13.4	8.1[d]	6.5	7.1, 4.7	6.1, 4.7
2018-04-27	16[c]	Influent	14	8.18	7.28	160	-
		Secondary Effluent	14.8	6.48	4.48	6.6, 6.7	4.3, 6.9
2018-06-26	21[c]	Influent	20	4.91	7.18	215	-
		Secondary Effluent	20.8	3.37	6.71	3.9	2.8
2018-08-13	24	Influent	22	2.68	7.06	160	-
		Primary Effluent	22	0.75	6.66	-	-
		Activated Sludge	22.8	0.35	6.31	-	-
		Secondary Effluent	23.2	2.82	6.53	4.8, 4.9	4.6, 3.9
		Final Effluent	22.5	6.42	6.59	4.8, 4.9	4.6, 3.9
2018-10-24	11	Influent	18.6	3.73	7.26	200	-
		Secondary Effluent	18	1.58	6.35	6.8, 5.6	4.2, 4.3

[a]TSS and BOD are measured in the final effluent approximately weekly at wastewater treatment facility. Final effluent measurements will be taken as secondary effluent measurements in this study.

[b]Weekly values provided before and after the sampling event, unless sampling coincided with weekly data point.

[c]Temperature taken from archived weather data available at time of sampling.

[d]Measurement taken from plant data.
[e]No recycling of activated sludge occurring due to high flow conditions caused by heavy periods of rainfall. No nitrification occurring.

Supplementary Table 2. Raw read and post-quality control (QC) sequence metrics performed via in MetaStorm (Arango-Argoty et al., 2016).

Sample_ID	Stage of Treatment	Raw Read Pairs	Read Pairs After QC	%Reads Pairs Passing QC
17-DEC-IN	Influent	37366657	36449253	97.54
17-DEC-SE	Secondary Effluent	37038559	36069946	97.38
17-JUL-IN	Influent	35676038	34847071	97.68
17-JUL-SE	Secondary Effluent	38373440	37342749	97.31
17-OCT-IN	Influent	43579744	42695000	97.97
17-OCT-SE	Secondary Effluent	44250971	43125445	97.46
18-APR-IN	Influent	26192397	25628288	97.85
18-APR-SE	Secondary Effluent	40754048	39785292	97.62
18-AUG-AS	Activated Sludge	29835249	29140007	97.67
18-AUG-FE	Final Effluent	44511900	43285007	97.24
18-AUG-IN	Influent	28703438	28006923	97.57
18-AUG-PE	Primary Effluent	54498571	53259913	97.73
18-AUG-SE	Secondary Effluent	35155619	34313756	97.61
18-FEB-AS	Activated Sludge	45702582	44316672	96.97
18-FEB-FE	Final Effluent	34810818	33948558	97.52
18-FEB-IN	Influent	43601844	42551990	97.59
18-FEB-PE	Primary Effluent	29338422	28671670	97.73
18-FEB-SE	Secondary Effluent	42808929	41843448	97.74
18-JUN-IN	Influent	46660742	45691625	97.92
18-JUN-SE	Secondary Effluent	41261213	40328173	97.74
18-OCT-IN	Influent	3736000	3651048	97.73
18-OCT-SE	Secondary Effluent	37820256	36922790	97.63

Supplementary Table 3. List of 61 category 3 (increased in all sample events) ARGs.

ARGs
*aad*A2
*aad*A8
*abe*M
*acr*B
*acr*D
*acr*F
*ade*B
*ade*I
*ade*J
*ade*K
*bla*AER-1
aph(3")-Ib
aph(6)-Id
*arn*A
*bac*A
*bae*R
*bae*S
*cml*A5
*cpx*A
crp
*dfr*A3
*emr*A
*emr*B
*emr*D
*acr*A in *Enterobacter cloacae*
*erm*B
lamb in *Escherichia coli*
*mdf*A in *Escherichia coli*
*gol*S
*omp*K35 in *Klebsiella pneumoniae*
*omp*K36 in *Klebsiella pneumoniae*
*mds*B
*mds*C
*mdt*A
*mdt*H
*mef*C
mel
*mex*A
*mex*L
*mph*D
*mph*G
*msr*E
*mva*T
*opm*H
*opr*J
*bla*OXA-16

Supplementary Table 4. ANOSIM pairwise tests for relative abundance of all antibiotic resistance genes across all treatment processes.

Groups (n[a])	R-statistic	Significance level, *p*
Influent (n=8), Secondary Effluent (n=8)	0.933	0.001
Influent (n=8), Activated Sludge (n=2)	1	0.022
Influent (n=8), Final Effluent (n=2)	1	0.022
Influent (n=8), Primary Effluent (n=2)	0.228	0.178
Secondary Effluent (n=8), Activated Sludge (n=2)	0.151	0.267
Secondary Effluent (n=8), Final Effluent (n=2)	-0.306	0.911
Secondary Effluent (n=8), Primary Effluent (n=2)	0.776	0.022
Activated Sludge (n=2), Final Effluent (n=2)	0.25	0.333
Activated Sludge (n=2), Primary Effluent (n=2)	1	0.333
Final Effluent (n=2), Primary Effluent (n=2)	1	0.333

[a]n = number of samples within group

Supplementary Table 5. ANOSIM pairwise tests for all genus level relative abundance across all treatment processes.

Groups (n[a])	R-statistic	Significance level, *p*
Influent (n=8), Secondary Effluent (n=8)	0.801	0.002
Influent (n=8), Activated Sludge (n=2)	1	0.019
Influent (n=8), Final Effluent (n=2)	1	0.024
Influent (n=8), Primary Effluent (n=2)	0.31	0.136
Secondary Effluent (n=8), Activated Sludge (n=2)	0.289	0.15
Secondary Effluent (n=8), Final Effluent (n=2)	-0.172	0.795
Secondary Effluent (n=8), Primary Effluent (n=2)	0.547	0.03
Activated Sludge (n=2), Final Effluent (n=2)	0.25	0.667
Activated Sludge (n=2), Primary Effluent (n=2)	1	0.333
Final Effluent (n=2), Primary Effluent (n=2)	0.75	0.333

[a]n = number of samples within group

Supplementary Table 6. Assembly information presented in MetaStorm (Arango-Argoty et al., 2016). Values determined to calculate relative risk scores using MetaCompare (Oh et al, 2018).

Sample	Percent Assembled	#Contigs	#ARG	#MGE	#PAT	Q(ARG)	Q(ARG_MGE)	Q(ARG_MGE_PAT)	Risk Score
17-DEC-IN	43	654151	3594	8295	13043	0.00549414	0.00023542	0.00006268	36.46
17-DEC-SE	54	587366	849	4993	501	0.00144544	0.00010896	0.00001192	21.37
17-JUL-IN	41	630444	3210	7458	12498	0.00509165	0.00023317	0.00007138	34.89
17-JUL-SE	69	315513	540	2804	362	0.0017115	0.0001553	0.00000951	22.26
17-OCT-IN	43	749710	4118	9332	20201	0.00549279	0.0002561	0.00008403	36.83
17-OCT-SE	58	525930	924	3497	714	0.00175689	0.00011408	0.00003042	22.32
18-APR-IN	43	463657	2425	5967	6815	0.00523016	0.00022215	0.00004961	35.18
18-APR-SE	57	507711	756	3697	441	0.00148904	6.89E-05	0.00000788	21.35
18-AUG-AS	48	478979	1032	4654	589	0.00215458	0.00010856	0.00001044	23.38
18-AUG-FE	51	572315	1190	4419	1226	0.00207927	0.00010833	1.92E-05	23.19
18-AUG-IN	39	515184	2430	5791	7360	0.00471676	0.00020963	0.00005241	33.08
18-AUG-PE	39	964871	3899	9467	13041	0.00404095	0.00015961	0.00004975	30.14
18-AUG-SE	53	479626	921	3548	916	0.00192025	9.59E-05	0.00002502	22.7
18-FEB-AS	59	627702	1204	7677	684	0.00191811	0.00016409	0.00001593	22.91

18-FEB-FE	59	446325	794	4527	504	0.00177897	0.00012099	0.00000896	22.33
18-FEB-IN	44	778402	3151	9131	10364	0.00404804	0.00017472	0.00003469	30.17
18-FEB-PE	41	523362	2467	6071	11520	0.00471375	0.00021591	0.00005923	33.16
18-FEB-SE	53	494224	842	5232	516	0.00170368	0.00013961	0.00001619	22.2
18-JUN-IN	42	819981	4211	9617	17676	0.00513548	0.00024025	0.00009147	35.29
18-JUN-SE	50	504902	1062	4478	1505	0.00210338	0.00019014	0.00004357	23.66
18-OCT-IN	34	74873	368	1265	866	0.00491499	0.00030719	8.01E-05	34.83
18-OCT-SE	24	14876	9	21	8	0.000605	0	0	18.92

Supplementary Table 7. Clinically-relevant ARGs in each resistome.

Resistome Type (number of clinically-relevant ARGs out of total ARGs in specific resistome)	List of clinically-relevant ARGs present
Core of influent and secondary effluent (11/143)	*bla*OXA-3, *bla*OXA-5, *bla*OXA-16, *bla*OXA-46, *bla*OXA-74, *bla*OXA-118, *bla*OXA-129, *bla*OXA-145, *bla*OXA-205, *bla*OXA-210, *qnr*S2
Discriminatory (4/32)	*bla*GES-22, *bla*OXA-212, *bla*OXA-309, *bla*OXA-333

Supplementary Table 8. Concentrations (ng/L) of antibiotics detected in influent and final effluent samples. Values in parentheses are the proposed no effect concentration (PNEC) (Bengtsson-Palme & Larsson, 2016) below which no selection of antibiotic resistance bacteria is anticipated. Bold font reflects antibiotic concentrations greater than the PNEC.

Sampling Event	Stage of Treatment	MLS							
		A-ERY (1000 ng/L)	**AZI (250 ng/L)**	**CLA (250 ng/L)**	**ERY (1000 ng/L)**	**ROX (1000 ng/L)**	**SPI I (500 ng/L)[a]**	**SPI II**	**SPI III**
July 2017	Influent	64.44	140.30	43.35	n.d.	n.d.	n.d.	n.d.	n.d.
	Final Effluent	50.27	182.09	44.33	n.d.	n.d.	n.d.	n.d.	n.d.
October 2017	Influent	339.25	**2270.39**	n.d.	n.d.	n.d.	n.d.	n.d.	n.d.
	Final Effluent	152.09	**3586.24**	n.d.	n.d.	n.d.	n.d.	n.d.	n.d.
December 2017	Influent	n.d.	**6842.01**	n.d.	n.d.	n.d.	n.d.	n.d.	n.d.
	Final Effluent	335.59	**6169.65**	n.d.	n.d.	n.d.	n.d.	n.d.	n.d.
February 2018	Influent	n.d.	202.05	155.21	n.d.	n.d.	n.d.	n.d.	n.d.
	Final Effluent	22.76	**373.49**	165.24	n.d.	n.d.	n.d.	n.d.	n.d.
April 2018	Influent	n.d.	n.d.	**694.49**	n.d.	n.d.	n.d.	n.d.	n.d.
	Final Effluent	n.d.	n.d.	**1082.52**	n.d.	n.d.	n.d.	n.d.	n.d.
June 2018	Influent	n.d.	n.d.	16.89	n.d.	n.d.	n.d.	n.d.	n.d.
	Final Effluent	55.56	**422.08**	40.48	n.d.	n.d.	n.d.	n.d.	n.d.
August 2018	Influent	n.d.	**648.73**	n.d.	n.d.	n.d.	n.d.	n.d.	n.d.
	Final Effluent	22.46	**419.75**	n.d.	n.d.	n.d.	n.d.	n.d.	n.d.
October 2018	Influent	**1564.22**	**479.63**	**425.71**	n.d.	n.d.	n.d.	n.d.	n.d.
	Final Effluent	n.d.	**469.64**	220.69	n.d.	n.d.	n.d.	n.d.	n.d.

[a]PNEC established for spiramycin, not specifically spiramycin I, II, or III.

QUINOLONE						TETRACYCLINE				OTHER
CIP (64 ng/L)	**ENRO (64 ng/L)**	**NOR (500 ng/L)**	**OXO**	**SARA**	**TIL (1000 ng/L)**	**ATC**	**CTC**	**OTC**	**TET (1000 ng/L)**	**TYL (4000 ng/L)**
768.31	n.d.	n.d.	n.d.	n.d.	n.d.	n.d.	n.d.	n.d.	n.d.	n.d.
156.22	n.d.	n.d.	n.d.	n.d.	n.d.	n.d.	n.d.	n.d.	n.d.	n.d.
1688.42	n.d.	n.d.	n.d.	n.d.	n.d.	n.d.	n.d.	n.d.	n.d.	n.d.
161.70	n.d.	n.d.	n.d.	n.d.	n.d.	n.d.	n.d.	n.d.	n.d.	n.d.
2174.61	n.d.	n.d.	n.d.	n.d.	n.d.	n.d.	n.d.	n.d.	n.d.	n.d.
277.05	n.d.	n.d.	n.d.	n.d.	n.d.	n.d.	n.d.	n.d.	n.d.	n.d.
6314.85	n.d.	n.d.	n.d.	n.d.	n.d.	n.d.	n.d.	n.d.	n.d.	n.d.
453.28	n.d.	n.d.	n.d.	n.d.	n.d.	n.d.	n.d.	n.d.	n.d.	n.d.
1746.15	n.d.	n.d.	n.d.	n.d.	n.d.	n.d.	n.d.	n.d.	n.d.	n.d.
356.92	n.d.	n.d.	n.d.	n.d.	n.d.	n.d.	n.d.	n.d.	n.d.	n.d.
770.45	n.d.	n.d.	n.d.	n.d.	n.d.	n.d.	n.d.	n.d.	n.d.	n.d.
235.65	n.d.	n.d.	n.d.	n.d.	n.d.	n.d.	n.d.	n.d.	n.d.	n.d.
n.d.	n.d.	n.d.	n.d.	n.d.	n.d.	n.d.	n.d.	n.d.	n.d.	n.d.
n.d.	n.d.	n.d.	n.d.	n.d.	n.d.	n.d.	n.d.	n.d.	n.d.	n.d.
2178.37	n.d.	n.d.	n.d.	n.d.	n.d.	n.d.	n.d.	n.d.	n.d.	n.d.
434.52	n.d.	n.d.	n.d.	n.d.	n.d.	n.d.	n.d.	n.d.	n.d.	n.d.

SULFONAMIDE										TRIMETHOPRIM
A-SMX	**SCP**	**SPD**	**SDM**	**SMR**	**SMZ**	**SMI**	**SMX (16000 ng/L)**	**SMT**	**STZ**	**TMP (500 ng/L)**
916.89	n.d.	n.d.	n.d.	n.d.	n.d.	n.d.	284.44	n.d.	n.d.	396.08
73.12	n.d.	n.d.	n.d.	n.d.	n.d.	n.d.	71.78	n.d.	n.d.	466.87
2863.64	n.d.	n.d.	n.d.	n.d.	n.d.	n.d.	n.d.	n.d.	n.d.	**994.39**
109.11	n.d.	n.d.	n.d.	n.d.	n.d.	n.d.	228.60	n.d.	n.d.	353.59
2331.33	n.d.	n.d.	n.d.	n.d.	n.d.	n.d.	697.91	n.d.	n.d.	**538.31**
n.d.	n.d.	n.d.	n.d.	n.d.	n.d.	n.d.	452.21	n.d.	n.d.	430.50
3400.31	n.d.	n.d.	n.d.	n.d.	n.d.	n.d.	929.16	n.d.	n.d.	**1778.67**
n.d.	n.d.	n.d.	n.d.	n.d.	n.d.	n.d.	406.77	n.d.	n.d.	**1031.63**
750.80	n.d.	n.d.	n.d.	n.d.	n.d.	n.d.	576.18	n.d.	n.d.	**537.27**
n.d.	n.d.	n.d.	n.d.	n.d.	n.d.	n.d.	571.56	n.d.	n.d.	**830.93**
3059.79	n.d.	n.d.	n.d.	n.d.	n.d.	n.d.	901.93	n.d.	n.d.	**604.57**
n.d.	n.d.	n.d.	n.d.	n.d.	n.d.	n.d.	364.92	n.d.	n.d.	**576.19**
2162.70	n.d.	n.d.	n.d.	n.d.	n.d.	n.d.	5787.09	n.d.	n.d.	**978.69**
84.74	n.d.	n.d.	n.d.	n.d.	n.d.	n.d.	3883.24	n.d.	n.d.	**833.31**
3053.07	n.d.	n.d.	n.d.	n.d.	n.d.	n.d.	n.d.	n.d.	n.d.	**1744.75**
37.28	n.d.	n.d.	n.d.	n.d.	n.d.	n.d.	192.13	n.d.	n.d.	311.32

Abbreviations: **MLS** = macrolide-lincosamide-streptogramin; **A-ERY** = anyhdro erythromycin; **AZI** = azithromycin; **CLA** = clarithromycin; **ERY** = erythromycin; **ROX** = roxithromycin; **SPI I** = spiramycin I; **SPI II** = spiramycin II; **SPI III** = spiramycin III; **CIP** = ciprofloxacin; **ENRO** = enrofloxacin; **NOR** = norfloxacin; **OXO** = oxolinic acid; **SARA** = sarafloxacin; **TIL** = tilmicosin; **ATC** = anhydrochlorotetracycline; **CTC** = chlorotetracycline; **OTC** = oxytetracycline; **TET** = tetracycline; **TYL** = tylosin; **A-SMX** = acetylsulfamethoxazole; **SCP** = sulfachloropyrazidine; **SPD** = sulfadiazine; **SDM** = sulfamethoxine; **SMR** = sulfamerazine; **SMZ** = sulframethazine; **SMI** = sulfamethizole; **SMX** = sulfamethoxazole; **SMT** = sulfamethoxydiazine; **STZ** = sulfathiazole; **TMP** = trimethroprim